

The Inhomogeneous Fermi-Pasta-Ulam Chain, a Case Study of the 1 : 2 : 3 Resonance

Roelof Bruggeman¹ · Ferdinand Verhulst¹ 

Received: 30 November 2016 / Accepted: 28 June 2017 / Published online: 2 August 2017
© The Author(s) 2017. This article is published with open access at Springerlink.com

Abstract A 4-particles chain with different masses represents a natural generalization of the classical Fermi-Pasta-Ulam chain. It is studied by identifying the mass ratios that produce prominent resonances. This is a technically complicated problem as we have to solve an inverse problem for the spectrum of the corresponding linearized equations of motion. In the case of such an inhomogeneous periodic chain with four particles each mass ratio determines a frequency ratio for the quadratic part of the Hamiltonian. Most prominent frequency ratios occur but not all. In general we find a one-dimensional variety of mass ratios for a given frequency ratio.

A detailed study is presented of the resonance 1 : 2 : 3. A small cubic term added to the Hamiltonian leads to a dynamical behaviour that shows a difference between the case that two opposite masses are equal and a striking difference with the classical case of four equal masses. For two equal masses and two different ones the normalized system is integrable and chaotic behaviour is small-scale. In the transition to four different masses we find a Hamiltonian-Hopf bifurcation of one of the normal modes leading to complex instability and Shilnikov-Devaney bifurcation. The other families of short-periodic solutions can be localized from the normal forms together with their stability characteristics. For illustration we use action simplices and examples of behaviour with time.

Keywords Inhomogeneous FPU · 1 : 2 : 3 resonance · Hamiltonian-Hopf · Symmetry

Mathematics Subject Classification 70H07 · 70H12 · 34E10 · 37J40

1 Introduction

The Fermi-Pasta-Ulam (FPU) chain or lattice is an n degrees-of-freedom (dof) Hamiltonian system that models a chain of oscillators with nearest-neighbour interaction, see [7] and

✉ F. Verhulst
f.verhulst@uu.nl

R. Bruggeman
r.w.bruggeman@uu.nl

¹ Mathematisch Instituut, Utrecht University, PO Box 80.010, 3508TA Utrecht, Netherlands

[8]. We will describe the model in Sect. 2. There exists a huge amount of literature on the FPU chain but nearly always regarding the classical case of equal masses, see for recent references [4]. One should note that, although the classical case looks physically natural, its dynamics is non-generic because of symmetries. One of the consequences is that only two dof resonances are effective in such a chain with n particles; see [13]. In the conclusions we will mention applications and make some observations about the classical FPU chain in the light of the present analysis.

In this paper we will outline a research program to study the case where the masses are different. An inhomogeneous nonlinear lattice with nearest neighbour interaction is studied in [15] with emphasis on energy control. The case of alternating masses was studied in [9] for a FPU chain to obtain insight in the equipartition of energy. A preliminary but important conclusion in [9] is that for the masses considered and on long timescales no equipartition takes place. This has been confirmed by analysis based on symmetries and normal forms in [3].

It is understandable that only a few results were obtained for inhomogeneous lattices as the choice of inhomogeneities, the masses of the lattice, seems to be arbitrary. We will solve this arbitrariness by focusing on the presence of resonances induced by the choice of masses. After referring to some basic material on Hamiltonians and normal forms we formulate in Sect. 2 the periodic FPU α chain with arbitrary (positive) masses. In such a n degrees-of-freedom system there exists a momentum integral that enables us to reduce to a $n - 1$ dof system. An inverse problem is considered in Sect. 3: how do we find mass distributions producing prominent resonances in the spectrum induced by $H_2(p, q)$, the quadratic part? This involves the analysis of the inverse map of the vector of mass distribution to the vector of positive eigenvalues of an associated coefficient matrix. This problem is solved in Sect. 3 for the cases of 3 and 4 particles; in the latter case it turns out that of the four 1st order resonances that exist in general (see for the terminology [14]) 3 exist, of the 12 possible 2nd order resonances 10 exist in this FPU chain. In Sect. 4 we focus on the 1 : 2 : 3 resonance that arises for a one-dimensional variety of mass ratios. It turns out that for one particular combination of mass ratios, the normal form of the nonlinear system is integrable. Moving from this particular case into the variety of mass ratios, one of the periodic solutions shows Hamilton-Hopf bifurcation that corresponds with Shilnikov-Devaney bifurcation in this Hamiltonian system and produces a chaotic normal form.

In the conclusions we draw attention to possible applications of the present paper.

The Appendix contains general statements on the relation between mass ratios and the spectrum induced by $H_2(p, q)$ that can be useful for future research. Table 3 summarises the instructions for the case of 4 particles. It is shown that for a given n -dimensional eigenvector characterizing the FPU chain, all positive solutions of an n -dimensional mass distribution are in a compact subset of \mathbb{R}^n . This subset is empty in some cases, for instance the important 1 : 1 : ... : 1 resonance does not arise for the periodic FPU α chain with four or more particles.

1.1 Hamiltonian Formulation

For an autonomous Hamiltonian system with n dof, n independent integrals suffice for integrability, in that case there will be no chaotic motion in such a system. However, in general, Hamiltonian systems with two or more dof are non-integrable. In many cases, this phenomenon was identified with homoclinic chaos as predicted by Poincaré in the nineteenth century, see [11, vol. 3]; for a description see [17, Sects. 5.4 and 9.3].

In the seventies of last century, a number of scientists started with the computation and analysis of normal forms of general Hamiltonian systems near equilibrium. Introductions

and surveys of results can be found in [14, Chap. 10] and [18]. We will follow the same terminology.

In the sequel, a periodic solution should be understood as a periodic solution for a fixed value of the energy (iso-energetic solution), so actually it corresponds for the full Hamiltonian system with a family of periodic solutions parameterized by the energy.

Normal form computations for Hamiltonian systems can be carried out in various ways. Apart from efficiency, the main point is to keep the system energy-preserving and preferably canonical. Using for instance polar coordinates like action-angle coordinates or amplitude-phase coordinates one can perform averaging over the angles or explicitly time to obtain a first-order normal form. One may consult [14] or [18] for more details. An introductory text is [16, Chaps. 11 and 12].

In Sect. 4 we will analyze periodic α -chains (FPU chains where the Hamiltonian is truncated after the cubic terms), containing the $1 : 2 : 3$ resonance with main objective to investigate the stability of the short-periodic solutions on the energy manifold and the integrability of the normal form. This is highly relevant for the characterization of the chaotic dynamics of the system but, as mentioned above, it raises special problems. In the cases of vanishing actions or amplitudes, for instance when studying normal modes, the procedure will be as follows (see also Sect. 4.1). Starting with the equations of motion, we will use co-moving coordinates (see for instance transformation (11.9-10) in Chap. 11 of [16]) to obtain a first order normal form. This normal form is used to localize the short-periodic solutions; the normal form conserves the energy but the transformation is not canonical. We will use averaging-normalization as it yields rigorous approximation results (see [14]), the results are qualitatively and quantitatively precise. The same holds when we use polar coordinates outside the coordinate planes.

In Sect. 4, the short-periodic solutions can be computed explicitly. The next step is then to linearize near the periodic solutions and to determine the Floquet exponents for which we have to study coupled Mathieu equations. This is still a formidable task, but we can obtain a first order approximation of the exponents by normalizing the coupled Mathieu equations. This will give a number of spectral stability results in Sect. 4.

In the [Appendix](#) we outline the general procedure to obtain mass ratios that correspond with resonance. We also give indications of the extension to periodic FPU chains with n particles.

1.2 Outline of a Research Programme

The original Fermi-Pasta-Ulam chain [7] consists of n oscillators of equal mass with nearest-neighbour interaction. In a neighbourhood of equilibrium, the spectrum of the linear part of the equations of motion plays a crucial part regarding the nature of the ensuing dynamics, see for instance [14] or [18]. Considering inhomogeneous mass distributions in FPU chains, one can produce a great many different spectra induced by H_2 . Each of these cases may produce different dynamics in the corresponding FPU chain. In Sect. 3 we will consider resonant spectra for the case of three and more extensively four particles with periodic boundary conditions i.e. chains where the first and the last oscillator are connected. For the case of four particles we will focus on the rich dynamics of the $1 : 2 : 3$ resonance. An outline of possible further research follows here:

1. According to Table 1 regarding the case of four particles, we also have to study two first order resonances ($1 : 2 : 1$ and $1 : 2 : 4$) and ten second order resonances. Also, higher order resonances may be worthwhile to investigate. Special attention should be given to the $1 : 1 : 2$ and $1 : 1 : 3$ cases as only four special mass ratios produce these resonances.

- In such a case degenerations may arise so that we have to consider detuning phenomena, see [14].
2. Cases of five and more particles will present many more problems.
 3. The present study is restricted to so-called periodic α -chains. Including quartic terms in the Hamiltonian (β -chains) and considering lattices with fixed begin- and end-point will produce new results.
 4. The study presented here and possibly future studies will throw light on qualitative and quantitative differences between systems in nearest-neighbour interaction and non-local interaction, a topic that is relevant for plasma physics and stellar dynamics.

2 The Fermi-Pasta-Ulam Chain

For the mono-atomic case of the original periodic FPU-problem (all masses equal) it was shown in [12] for up to six degrees-of-freedom (dof) and much more general in [13], that the corresponding normal forms are governed by 1 : 1 resonances and that these Hamiltonian normal forms are integrable. This explains the recurrence phenomena near equilibrium, it also shows that the classical FPU chain has symmetries to make the problem non-generic.

We will drop the original assumption of identical (mono-atomic) particles to consider the periodic FPU-problem again. For n particles with mass $m_j > 0$, position q_j and momentum $p_j = m_j \dot{q}_j$, $j = 1 \dots n$, $\varepsilon \geq 0$ a small parameter, the Hamiltonian is of the form:

$$H(p, q) = \sum_{j=1}^n \left(\frac{1}{2m_j} p_j^2 + V(q_{j+1} - q_j) \right) \quad \text{with } V(z) = \frac{1}{2}z^2 + \varepsilon \frac{\alpha}{3}z^3 + \varepsilon^2 \frac{\beta}{4}z^4. \quad (1)$$

The quadratic part of the Hamiltonian is not in diagonal form; for $n = 3, 4 \dots$ the linearized equations of motion can be written as:

$$\begin{cases} m_1 \ddot{q}_1 + 2q_1 - q_2 - q_n & = 0, \\ m_2 \ddot{q}_2 + 2q_2 - q_3 - q_1 & = 0, \\ m_3 \ddot{q}_3 + 2q_3 - q_4 - q_2 & = 0, \\ \dots & = 0, \\ m_n \ddot{q}_n + 2q_n - q_1 - q_{n-1} & = 0. \end{cases} \quad (2)$$

We can write for the quadratic part of $H(p, q)$:

$$H_2 = \frac{1}{2} p^T A_n p + \frac{1}{2} q^T C_n q, \quad (3)$$

with A_n the $n \times n$ diagonal matrix with at position (i, i) the value $m_i^{-1} =: a_i$, C_n is an $n \times n$ matrix. For an analysis of the quadratic term $H_2(p, q)$ we need to know the eigenvalues of $A_n C_n$. The relation between the eigenvalues of $A_n C_n$ and the eigenvalues of the matrix of coefficients of system (2) will be given below. Since the null space of C_n has dimension one, the matrix $A_n C_n$ has an eigenvalue 0 corresponding to a (translational) momentum integral. It will turn out that the other eigenvalues of $A_n C_n$ are positive, as expected. For a given set of masses, the calculation of the remaining eigenvalues corresponding with the frequencies of the linearized system is easy, but we are faced with another, an inverse problem. To focus ideas, suppose that $n = 4$. The presence of the momentum integral implies that we have to

consider a three degrees-of-freedom (dof) Hamiltonian problem. We know, see for instance [14, Chap. 10] or [18], that the first order resonances are $1 : 2 : 1, 1 : 2 : 2, 1 : 2 : 3$ and $1 : 2 : 4$. The question is then if and how we can choose the masses so that these prominent resonances are present. Of course, this problem will be more formidable if $n > 4$. In the next section we determine for $n = 4$ the ratios of masses that produce the resonance $1 : 2 : 3$. The approach works equally well for other prescribed ratios of eigenvalues, as we discuss in the Appendix. Prominent resonances for $n > 4$ can be found but a systematic study of these cases poses a difficult open algebraic problem.

3 The Spectrum Induced by H_2

After a number of general considerations we will give details for the cases of three and four particles. The first case is rather trivial as far as the spectrum goes, the case of four particles is already quite complicated. Here we mention the main facts that we need in the later sections. In the Appendix we will give more details.

3.1 The Matrix for Inhomogeneous FPU-Lattices and Its Eigenvalues

The linear system (2) can be written as

$$\begin{pmatrix} \dot{q} \\ \ddot{q} \end{pmatrix} = M \begin{pmatrix} q \\ \dot{q} \end{pmatrix}, \quad \text{where } M = \begin{pmatrix} 0 & I_n \\ -A_n C_n & 0 \end{pmatrix}, \tag{4}$$

where the matrix A_n is a diagonal matrix with the inverse masses $m_j^{-1} =: a_j$ on the diagonal, and where the matrix C_n has elements 2 on the diagonal, and -1 at positions $(i, i + 1)$ and $(i, i - 1)$, with the indices taken modulo n . For instance,

$$C_5 = \begin{pmatrix} 2 & -1 & 0 & 0 & -1 \\ -1 & 2 & -1 & 0 & 0 \\ 0 & -1 & 2 & -1 & 0 \\ 0 & 0 & -1 & 2 & -1 \\ -1 & 0 & 0 & -1 & 2 \end{pmatrix}.$$

(This matrix turns up elsewhere in mathematics. It is the affine Cartan matrix of the completed root system A_n . See e.g. [2, Déf. 3 in 1.5 of Chap. 6, and Planche I].)

The $(2n) \times (2n)$ matrix M has a double eigenvalue 0, corresponding to the momentum integral

$$\sum_{j=1}^n m_j \dot{q}_j = \text{constant}. \tag{5}$$

In the sequel we will choose the case of vanishing momentum integral which is not a restriction of generality. If λ is a positive eigenvalue of $A_n C_n$, then $i\sqrt{\lambda}$ and $-i\sqrt{\lambda}$ are eigenvalues of M , corresponding to frequencies of eigenmodes of the linearized system. So it is useful to collect results concerning the eigenvalues of $A_n C_n$.

Proposition 3.1 *For $n = 3, 4 \dots$ the matrix $A_n C_n$ has one eigenvalue 0 and $n - 1$ positive eigenvalues $\lambda_1, \dots, \lambda_{n-1}$, possibly coinciding. If eigenvalues coincide the corresponding eigenspace has maximal dimension.*

Proof Since the $a_j = m_j^{-1}$ are positive, the matrix $A_n^{1/2}$ is well-defined. The symmetric matrix $A_n^{1/2}C_nA_n^{1/2}$ has real eigenvalues, and the algebraic and geometric multiplicities of eigenvalues coincide.

If y is an eigenvector of A_nC_n with eigenvalue λ , then $\lambda A_n^{-1}y = C_ny$, and the scalar product with y for both sides of the equation gives the equality

$$\lambda \sum_i a_i^{-1}y_i^2 = 2 \sum_i y_i^2 - 2 \sum_i y_iy_{i-1}.$$

(Indices taken modulo n .) So

$$\sum_i (2 - \lambda/a_i)y_i^2 = 2 \sum_i y_iy_{i-1}.$$

With Schwarz’s inequality applied to the vector (y_i) and the vector (y_{i-1}) this implies $\lambda \geq 0$. Equality occurs only if the vectors (y_i) and (y_{i-1}) are positive multiples of each other, which occurs only for multiples of $(1, 1, \dots, 1)$. □

For the investigation of the linearized problem we need to understand the map $\mathbb{R}_{>0}^n \rightarrow \mathbb{R}_{>0}^{n-1}$, from a vector (a_1, \dots, a_n) of inverse masses to a vector $(\lambda_1, \dots, \lambda_{n-1})$ of positive eigenvalues. The order of the eigenvalues is not determined, so we have, more precisely, a map $\rho_n : \mathbb{R}_{>0}^n \rightarrow S_{n-1} \backslash \mathbb{R}_{>0}^{n-1}$, with the action of the symmetric group S_{n-1} on the coordinates. For the linearized inhomogeneous FPU-chain described by system (2), the dihedral group D_n with $2n$ elements permutes the coordinate q_j (generated by a shift and a reflection). This transforms system (2) into an equivalent system. Another symmetry is by scaling: $\rho(t(a_1, \dots, a_n)) = t\rho(a_1, \dots, a_n)$ for $t > 0$.

To investigate the correspondence between eigenvalues and inverse masses we use the equality

$$\det(A_nC_n - \lambda I_n) = -\lambda \prod (\lambda_j - \lambda),$$

for $(\lambda_1, \dots, \lambda_{n-1}) = \rho(a_1, \dots, a_n)$. Comparing the coefficients of this polynomial we obtain the equalities

$$p_j(A_n) = e_{n-j}(\{\lambda_1, \dots, \lambda_{n-1}\}) \quad (1 \leq j \leq n - 1), \tag{6}$$

with the elementary symmetric functions e_k and homogeneous polynomials $p_j(A_n)$ in the a_j of degree $n - j$. This describes the structure of the set of diagonal matrices A_n for a prescribed spectrum of A_nC_n . It is the set of points with positive coordinates in an algebraic set in \mathbb{C}^n which is the intersection of $n - 1$ hyperplanes given by equations of degree $1, 2, \dots, n - 1$.

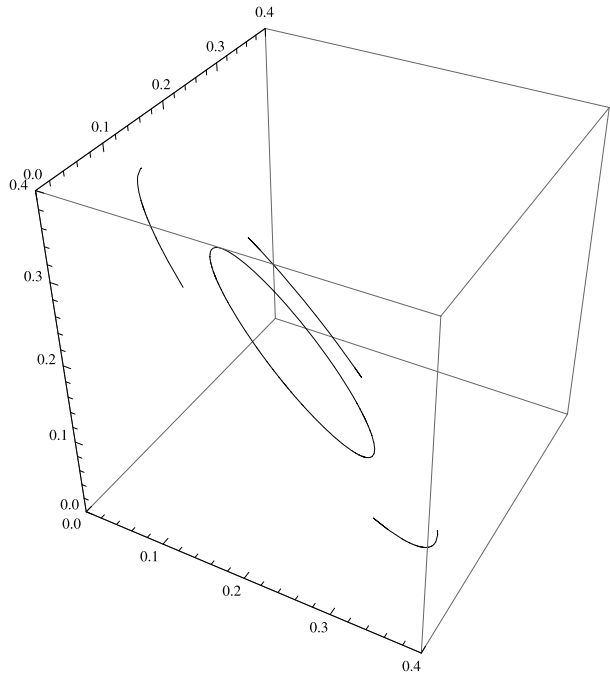
In Lemma A.2 in the Appendix we’ll show that

$$p_{n-1}(A_n) = 2 \sum_i a_i, \quad p_{n-2}(A_n) = \sum_{1 \leq i < j \leq n} c_{i,j} a_i a_j, \tag{7}$$

with $c_{i,j} = 3$ if $i - j = \pm 1 \pmod n$, and $c_{i,j} = 4$ otherwise. All $p_j(A_n)$ are invariant under the action of the dihedral group D_n on the coordinates a_j .

In the Appendix we will also show that all real solutions (a_1, \dots, a_n) for a given eigenvalue vector $(\lambda_1, \dots, \lambda_{n-1})$ are in a compact subset of \mathbb{R}^n . This subset may be empty. For all $n \geq 4$ the $1 : 1 : \dots : 1$ resonance does not occur for any mass distribution.

Fig. 1 Solutions sets of inverse masses (a_1, a_2, a_3) for the FPU-chain with three particles. For the eigenvalue ratio $\lambda_1/\lambda_2 = 2$ of matrix $A_n C_n$ the solution set is compact; it is an ellipse in $\mathbb{R}_{>0}^3$. For the eigenvalue ratio $\lambda_1/\lambda_2 = 4$ the solutions are on a larger ellipse in \mathbb{R}^3 , which intersects $\mathbb{R}_{>0}^3$ in three open curves



3.2 The Case of Three Particles

For $n = 3$ the determination of the eigenvalues for given inverse masses amounts to solving the quadratic equation

$$\lambda^2 - 2(a_1 + a_2 + a_3)\lambda + 3(a_1a_2 + a_1a_3 + a_2a_3) = 0,$$

which has positive solutions.

Conversely, for all choices (λ_1, λ_2) of positive eigenvalues, values of a_1, a_2, a_3 can be found such that $A_3 C_3$ has eigenvalues λ_1, λ_2 and 0. If $\lambda_1 = \lambda_2$ there is exactly one solution $a_1 = a_2 = a_3 = \frac{1}{3}\lambda$ (equal masses). If the eigenvalues have ratio $\lambda_1/\lambda_2 > 1$ then the corresponding points (a_1, a_2, a_3) in \mathbb{R}^3 form an ellipse. This ellipse may or may not be contained in the positive octant. See Fig. 1.

3.3 The Case of Four Particles

In the case $n = 4$ we use the scaling to restrict our further investigation to eigenvalues satisfying $\lambda_1 + \lambda_2 + \lambda_3 = 1$. Working out the polynomials in (6) for the case $n = 4$ we obtain three equations for a given vector $(\lambda_1, \lambda_2, \lambda_3) \in \mathbb{R}_{>0}^3$:

$$\begin{aligned} 4(a_1a_2a_3 + a_2a_3a_4 + a_3a_4a_1 + a_4a_1a_2) &= \lambda_1\lambda_2\lambda_3 =: \xi, \\ 3(a_1a_2 + a_2a_3 + a_3a_4 + a_4a_1) + 4(a_1a_3 + a_2a_4) &= \lambda_1\lambda_2 + \lambda_2\lambda_3 + \lambda_3\lambda_1 =: \eta, \quad (8) \\ 2(a_1 + a_2 + a_3 + a_4) &= 1. \end{aligned}$$

Table 1 Fibers of resonances

Ratio	Fiber	Ratio	Fiber
$(1 : 1 : \sqrt{2})$	One point (classical case $A_4 = I_4$)		
Resonances of order 1			
$(1 : 1 : 2)$	four points	$(1 : 2 : 2)$	empty
$(1 : 2 : 3)$	four open curves	$(1 : 2 : 4)$	12 open curves
Resonances of order 2			
$(1 : 1 : 1)$	empty	$(1 : 1 : 3)$	four points
$(1 : 2 : 5)$	12 open curves	$(1 : 2 : 6)$	12 open curves
$(1 : 3 : 3)$	empty	$(1 : 3 : 4)$	four open curves
$(1 : 3 : 5)$	four open curves	$(1 : 3 : 6)$	12 open curves
$(1 : 3 : 7)$	12 open curves	$(1 : 3 : 9)$	12 open curves
$(2 : 3 : 4)$	two compact curves	$(2 : 3 : 6)$	two compact curves

We call the set of $(a_1, \dots, a_4) \in \mathbb{R}_{>0}^4$ satisfying these relations the *fiber* of $(\xi, \eta) \in \mathbb{R}_{>0}^2$. In Proposition A.5 in the Appendix we will give a precise characterization of the set of (ξ, η) for which the fiber is non-empty.

The resonances deserve special attention. A resonance $n_1 : n_2 : n_3$ in the linearized system (2) corresponds to an eigenvalue vector of A_4C_4 with the ratios $n_1^2 : n_2^2 : n_3^2$. We considered all resonances of order one and two, and obtained the results in Table 1. As noted in Sect. 1.2, the resonances $1 : 1 : 2$ and $1 : 1 : 3$ need special attention.

In Sect. A.2.2 in the Appendix we describe how to determine the fiber explicitly by choosing an additional parameter and solve the system of equations (8). The idea is to determine successively quantities that are invariant under a decreasing sequence of subgroups of the dihedral group D_4 acting by permutation on the vector (a_1, a_2, a_3, a_4) .

3.4 The Resonance 1 : 2 : 3

Here we consider the resonance that is the subject of study in the next section.

By scaling we arrange $\lambda_1 = \frac{9}{14}$, $\lambda_2 = \frac{2}{7}$, $\lambda_3 = \frac{1}{14}$ to satisfy the last equation in (8). We follow the computational scheme in Table 3 in the Appendix. This leads to

$$\begin{aligned}
 a_1, a_3 &= \frac{2 + u}{56} \mp \frac{\sqrt{2}}{112} \sqrt{\frac{u(6 - u)(16 - u)}{5 - u}}, \\
 a_2, a_4 &= \frac{12 - u}{56} \mp \frac{1}{56\sqrt{2}} \sqrt{\frac{(6 + u)(4 - u)(10 - u)}{5 - u}},
 \end{aligned}
 \tag{9}$$

where we take the minus sign for a_1 and a_2 . The parameter u runs through the interval $[0, u_1)$ with

$$u_1 = \frac{8}{3} - \frac{2}{3} \sqrt[3]{19} \approx 0.887732.
 \tag{10}$$

Figure 2 gives a plot.

We get all solutions when we let the dihedral group D_4 act on the solutions that we constructed. The branch in Fig. 2 and its image under $[1, 3] \in D_4$ have the point parametrized by $u = 0$ in common.

Fig. 2 One branch of the fiber for the resonance 1 : 2 : 3 is given by the functions $a_1 \leq a_3 < a_2 < a_4$ on the interval $[0, u_1)$. (Horizontal axis: parameter u ; vertical axis: values of $a_j(u)$.) The three dots on the horizontal axis correspond to the values 0, 0.534105 and 0.826713 of the parameter u for which we will carry out simulations in the next section (the cases 0, 1 and 2)

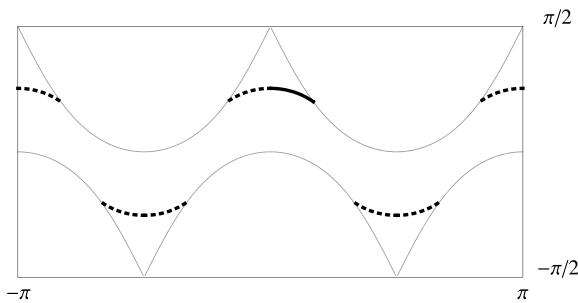
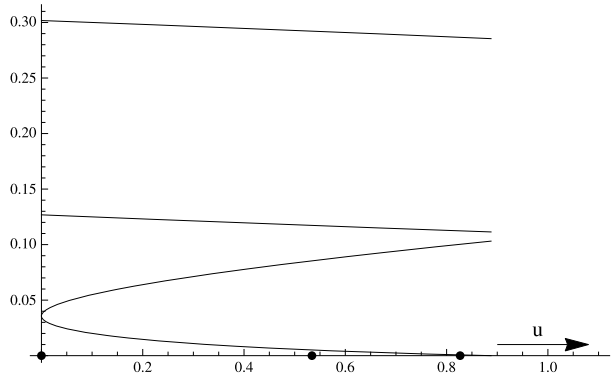


Fig. 3 The fiber for the resonance 1 : 2 : 3 is contained in an ellipsoid, which we describe in spherical coordinates. (Horizontally the azimuth ϕ , and vertically the inclination ψ . See (54).) The thick curve corresponds to the branch of the fiber in Fig. 2. The dotted curves correspond to the translates of this branch under the dihedral group D_4 . The thin curves indicate the boundary of the region corresponding to coordinates in $\mathbb{R}_{>0}^4$. The picture illustrates that the fiber for (1 : 2 : 3) consists of four open curves, and that (9) describes a fundamental domain for the action of the dihedral group on the fiber

3.5 Illustration of the Fiber

The equations in (9) describe a curve $u \mapsto (a_1(u), a_2(u), a_3(u), a_4(u))$ in $\mathbb{R}_{>0}^4$ corresponding to a one-parameter family of solutions for the inverse masses. To illustrate it we use the second and last equation in (8), which describe an ellipsoid in the hyperplane $a_1 + a_2 + a_3 + a_4 = \frac{1}{2}$. In (53) and (54) in the Appendix we'll describe this ellipsoid in a more explicit way. The first equation in (8) produces an intersection with this ellipsoid in some curves. The points with positive coordinates in this intersection form the fiber.

On this ellipsoid we can use a system of spherical coordinates, mapping the ellipsoid to the rectangle $[-\pi, \pi] \times [-\frac{1}{2}\pi, \frac{1}{2}\pi]$, with boundary identifications. The image of the fiber under this map is given in Fig. 3.

3.6 Transformation of the Hamiltonian

We form the diagonal matrix $A_4(u)$ with diagonal elements $a_j(u)$, $1 \leq j \leq 4$. In the proof of Proposition 3.1 we noted that $A_4(u)^{1/2}C_4A_4(u)^{1/2}$ is a symmetric matrix (as long as $u \in [0, u_1)$), so we can find an orthogonal matrix $U(u)$ such that $A_4(u)^{1/2}C_4A_4(u)^{1/2} = U(u)\Lambda U(u)^T$, where Λ is the diagonal matrix with diagonal elements $\frac{9}{14}$, $\frac{2}{7}$, $\frac{1}{14}$, and 0.

Then the transformation matrices

$$K(u) = A_4(u)^{-1/2}U(u), \quad L(u) = A_4(u)^{1/2}U(u) \tag{11}$$

determine a symplectic transformation

$$p = K(u)y, \quad q = L(u)x, \tag{12}$$

which transforms the quadratic part in (3) of the Hamiltonian into

$$H_2 = \frac{1}{2}y^T y + \frac{1}{2}x^T \Lambda x = \frac{1}{2} \sum_{j=1}^4 (y_j^2 + \lambda_j x_j^2). \tag{13}$$

This will produce the so-called quasi-harmonic form of the equations of motion. To see that H_2 takes the form (13) we need the existence of an orthogonal matrix $U(u)$ diagonalizing $A_4(u)^{1/2}C_4A_4(u)^{1/2}$. We do not need to know $U(u)$, $K(u)$ or $L(u)$ explicitly.

To transform the cubic and higher order terms of the Hamiltonian to coordinates corresponding to the eigenmodes of the linearized system we need to know the transformation matrix $L(u)$ explicitly. It is no problem to do this numerically with MATHEMATICA or MATLAB for any given $u \in [0, u_1)$. It is nicer to have $U(u)$, and hence $L(u)$ and $K(u)$, symbolically in terms of the parameter u . Lemma A.6 in the Appendix describes the method that we used to obtain a symbolic description.

For the cubic term we note that (with indices modulo 4)

$$\frac{1}{3} \sum_j (q_{j+1} - q_j)^3 = \sum_j (q_{j+1} - q_{j-1})q_j^2. \tag{14}$$

The substitution $(q_1, \dots, q_4)^T = L(u)(x_1, \dots, x_4)^T$ gives

$$H_3 = \varepsilon(d_1(u)x_1^3 + d_2(u)x_1^2x_2 + d_3(u)x_1^2x_3 + d_4(u)x_2^2x_1 + d_5(u)x_3^2x_1 + d_6(u)x_1x_2x_3 + d_7(u)x_2^3 + d_8(u)x_3^3 + d_9(u)x_3^2x_2 + d_{10}(u)x_2^2x_3), \tag{15}$$

with the functions d_j as indicated in Table 2.

4 The 1 : 2 : 3-Resonance for the Periodic α -Lattice ($n = 4$)

For any possible inhomogeneous FPU α -chain with four dof we have the system:

$$\begin{cases} \dot{q}_1 = v_1, \\ \dot{v}_1 = [-2q_1 + q_2 + q_4 - \varepsilon\alpha((q_1 - q_4)^2 - (q_2 - q_1)^2)]a_1, \\ \dot{q}_2 = v_2, \\ \dot{v}_2 = [-2q_2 + q_3 + q_1 - \varepsilon\alpha((q_2 - q_1)^2 - (q_3 - q_2)^2)]a_2, \\ \dot{q}_3 = v_3, \\ \dot{v}_3 = [-2q_3 + q_4 + q_2 - \varepsilon\alpha((q_3 - q_2)^2 - (q_4 - q_3)^2)]a_3, \\ \dot{q}_4 = v_4, \\ \dot{v}_4 = [-2q_4 + q_1 + q_3 - \varepsilon\alpha((q_4 - q_3)^2 - (q_1 - q_4)^2)]a_4, \end{cases} \tag{16}$$

Table 2 Coefficients of the cubic term of the Hamiltonian, transformed to eigenmodes, the so-called quasi-harmonic form. For $u = 0$ only d_3, d_6 and d_{10} are non-zero

$$\begin{aligned}
 d_1(u) &= \sqrt{u} \frac{27\sqrt{4-u}\sqrt{6-u}\sqrt{10-u}(16-u)(u+6)}{35840\sqrt{35}(5-u)}, \\
 d_2(u) &= -\sqrt{u} \frac{3\sqrt{3}\sqrt{10-u}\sqrt{16-u}\sqrt{u+6}(3u^2-30u+52)}{4480\sqrt{70}(5-u)}, \\
 d_3(u) &= -\frac{3\sqrt{3}\sqrt{4-u}\sqrt{6-u}\sqrt{16-u}\sqrt{u+6}(3u^2-30u+160)}{35840\sqrt{7}(5-u)}, \\
 d_4(u) &= -\sqrt{u} \frac{\sqrt{4-u}\sqrt{6-u}\sqrt{10-u}(-3u^2+30u+68)}{1120\sqrt{35}(5-u)}, \\
 d_5(u) &= -\sqrt{u} \frac{\sqrt{4-u}\sqrt{6-u}\sqrt{10-u}(3u^2-30u+64)}{7168\sqrt{35}(5-u)}, \\
 d_6(u) &= -\frac{-3u^4+60u^3-352u^2+520u+960}{2240\sqrt{14}(5-u)}, \\
 d_7(u) &= \sqrt{u} \frac{\sqrt{10-u}\sqrt{16-u}(6-u)(4-u)\sqrt{u+6}}{420\sqrt{210}(5-u)}, \\
 d_8(u) &= u \frac{\sqrt{4-u}\sqrt{6-u}\sqrt{16-u}(10-u)\sqrt{u+6}}{21504\sqrt{21}(5-u)}, \\
 d_9(u) &= -\sqrt{u} \frac{\sqrt{10-u}\sqrt{16-u}\sqrt{u+6}(u^2-10u+28)}{869\sqrt{210}(5-u)}, \\
 d_{10}(u) &= \frac{\sqrt{4-u}\sqrt{6-u}\sqrt{16-u}\sqrt{u+6}(u^2-10u+20)}{1120\sqrt{21}(5-u)}.
 \end{aligned}$$

The coefficient α has been retained for reference to the literature; here we will take $\alpha = 1$. If $a_1 = \dots = a_4 = 1$, we have the classical periodic FPU chain with four particles; it was shown in [12], that in this case the normal form is integrable. The implication is that for ε small, chaos is negligible in this classical case. The case of the 1 : 2 : 3-resonance is strikingly different as only if we have two masses equal, the normal form is integrable.

Apart from the Hamiltonian we have from (5) as a second (momentum) integral:

$$m_1 v_1 + m_2 v_2 + m_3 v_3 + m_4 v_4 = \text{constant}. \tag{17}$$

The presence of the momentum integral results in two zero eigenvalues of the matrix M in Eq. (4), so by reduction we have to deal essentially with a three dof system. This will be used and explicitly shown in the next three subsections.

According to Table 1 the 1 : 2 : 3 resonance is present among the possible inhomogeneous FPU lattices. Figure 2 gives one branch of values of inverse masses a_1, \dots, a_4 producing this resonance. All vectors (a_1, \dots, a_4) are obtained by the action of the dihedral group D_4 on the coordinates and the scaling $(a_1, \dots, a_4) \mapsto (ta_1, \dots, ta_4)$ with $t > 0$.

Table 1 and Fig. 2 show that the 1 : 2 : 3-resonance appears in one case with relatively well-balanced masses, two of which are equal. We denote this by case 0; it will turn out in Sect. 4.1 that this case is quite special dynamically. The other cases are less balanced regarding the masses. Case 0 corresponds to $u = 0$; as u increases (we have $0 \leq u < u_1$ with $u_1 = 0.887732$), the masses get less well-balanced, one of them tending to infinity. We study the dynamical behaviour in Sect. 4.2. For numerical simulations we have singled out two more cases indicated in Fig. 2.

The expression for the quadratic part of the Hamiltonian H_2 is:

$$H_2 = \frac{1}{2} \sum_{i=1}^4 a_i p_i^2 + \frac{1}{2} [(q_2 - q_1)^2 + (q_3 - q_2)^2 + (q_4 - q_3)^2 + (q_1 - q_4)^2]. \tag{18}$$

H_2 is a first integral of the linear system (2), it is also a first integral of the normal form of the full system (16). When using H_2 from the solutions of the truncated normal form

$$\tilde{H}(p, q) = H_2(p, q) + \varepsilon \tilde{H}_3(p, q),$$

we obtain an $O(\varepsilon)$ approximation of the (exact) $H_2(p(t), q(t))$ valid for all time; for a proof see [14, Chap. 10]. Note that in the equations we find it convenient to use the non-canonical velocities instead of the momenta. Using the expression $H_2(p(t), q(t))$ for the solutions of the full system (16) shows the accuracy of the normal form and gives an impression of the nature of the dynamics.

The normal form $\tilde{H}_3(p, q)$, written in action-angle coordinates or amplitude-phase coordinates (see below), will contain certain combination angles corresponding with the resonance. If \tilde{H}_3 contains only one combination angle, we have an additional integral of motion and the normal form $H_2 + \tilde{H}_3$ is integrable. In the case of two or more independent combination angles, we have to investigate the (non-)integrability of the normal form.

To display the quantitative aspects of the solutions we have the possibility of drawing an energy- or action-simplex or as an alternative to produce a time series for explicit solutions or integrals of the normal forms. Both techniques will be used.

As the short-periodic solutions have constant actions (or constant radii in polar coordinates), the integral H_2 of the normal form produces for fixed energy an action-simplex with short-periodic solutions represented by points; the actions τ_i and the polar coordinates r_i are related. One way of displaying the position of short-periodic solutions and their stability on the 5-dimensional energy manifold is the use of this action-simplex with normal modes at the vertices and solutions in the coordinate planes at the sides. The interior of the faces may contain short-periodic solutions in general position. Their stability is indicated by E (elliptic i.e. imaginary eigenvalues), H (hyperbolic i.e. real eigenvalues) and C (complex eigenvalues with real parts non-zero). See for instance for the action simplices displaying periodic solutions Fig. 6.

4.1 Case 0: The FPU Chain with Well-Balanced Masses

In this case we have the 1 : 2 : 3 resonance with mass values that are as much as possible similar; we have with $u = 0$ in (9):

$$a_1 = 0.0357143, \quad a_2 = 0.126804, \quad a_3 = 0.0357143, \quad a_4 = 0.301767.$$

Note that $a_1 = a_3$. We checked numerically that the time series $H_2(p(t), q(t))$ based on the original formulation of system (16) and the time series obtained from the transformed Hamiltonian (19) produce the same result as it should.

To put system (16) in the standard form of quasi-harmonic equations we have to apply the symplectic transformation $p = K(0)y, q = L(0)x$ in (12). This leads with (15) and Table 2 to the transformed Hamiltonian

$$H(y, x) = \frac{1}{2} \sum_{i=1}^4 (y_i^2 + \omega_i^2 x_i^2) + \varepsilon (d_3 x_1^2 + d_{10} x_2^2 + d_6 x_1 x_2) x_3, \tag{19}$$

with

$$\omega_1^2 = \frac{9}{14}, \quad \omega_2^2 = \frac{4}{14}, \quad \omega_3^2 = \frac{1}{14}, \quad \omega_4^2 = 0, \quad d_3 = -9\frac{\sqrt{21}}{490},$$

$$d_{10} = 2\frac{\sqrt{21}}{245}, \quad d_6 = -3\frac{\sqrt{14}}{490}.$$

Rescaling time $t/\sqrt{14} \rightarrow t$, the equations of motion for the three dof system become:

$$\begin{cases} \ddot{x}_1 + 9x_1 = -\varepsilon 14(2d_3x_1x_3 + d_6x_2x_3), \\ \ddot{x}_2 + 4x_2 = -\varepsilon 14(2d_{10}x_2x_3 + d_6x_1x_3), \\ \ddot{x}_3 + x_3 = -\varepsilon 14(d_3x_1^2 + d_{10}x_2^2 + d_6x_1x_2). \end{cases} \tag{20}$$

According to the Weinstein [20] result there exist at least three families of short-periodic solutions of system (20). Inspection of the equations provides us directly with one family given by:

$$x_1(t) = \dot{x}_1(t) = x_2(t) = \dot{x}_2(t) = 0, \quad \ddot{x}_3 + x_3 = 0. \tag{21}$$

For fixed energy we refer to this periodic solution as the x_3 normal mode; to find such an exact solution explicitly is slightly unusual, the solution is harmonic. Additional periodic solutions are obtained as approximations from normal forms as in [10]. In general, when normalizing a three dof system, one recovers the three actions and one expects to find the angles in combinations according to the actual resonances. For the 3 : 2 : 1 resonance these are to first order after normalization the so-called combination angles $\phi_1 - \phi_2 - \phi_3$ and $2\phi_3 - \phi_2$. At second order the combination angle $\phi_1 - 3\phi_3$ will arise etc., for details see Sect. 10.2.1 of [14]; for instance the term ‘genuine resonance’ associated with the so-called ‘annihilators’ of H_2 can be found in definition 10.2.2 of [14].

Computing the normal form ($H_2 + \varepsilon \bar{H}_3$) of system (20) to $O(\varepsilon)$ as in [10] or [14] and as we shall explicitly show below, only the d_6 term survives in \bar{H}_3 ; this makes the Hamiltonian (19) non-generic. An *intermediate normal form* of the equations of motion becomes:

$$\begin{cases} \ddot{x}_1 + 9x_1 = -\varepsilon 14d_6x_2x_3, \\ \ddot{x}_2 + 4x_2 = -\varepsilon 14d_6x_1x_3, \\ \ddot{x}_3 + x_3 = -\varepsilon 14d_6x_1x_2. \end{cases} \tag{22}$$

System (22) is called *intermediate* as it has still to be normalized, but the omitted terms play no part in the normalization to first order. There is a lot of freedom in choosing coordinate systems to compute the normal form of the equations of motion. Near the coordinate planes, in particular to study the stability of the normal modes, we will use co-moving coordinates. Away from the coordinate planes (solutions in general position), action-angle variables or polar coordinates are easier to handle than co-moving coordinates. For general position orbits we will use in system (20) transformations $x_i, \dot{x}_i \rightarrow r_i, \psi_i$ of the form:

$$x_i = r_i \cos(\omega_i t + \psi_i), \quad \dot{x}_i = -r_i \omega_i \sin(\omega_i t + \psi_i). \tag{23}$$

The actions τ_i are related to the r_i^2 , the angles ϕ_i to the arguments $(\omega_i t + \psi_i)$. Putting $\chi = \psi_1 - \psi_2 - \psi_3$ and averaging over time t , the averaging-normal form equations outside

the coordinate planes become:

$$\begin{cases} \dot{r}_1 = \varepsilon \frac{7}{6} d_6 r_2 r_3 \sin \chi, \\ \dot{r}_2 = -\varepsilon \frac{7}{4} d_6 r_1 r_3 \sin \chi, \\ \dot{r}_3 = -\varepsilon \frac{7}{2} d_6 r_1 r_2 \sin \chi, \\ \dot{\chi} = \varepsilon \frac{7}{2} d_6 \frac{\cos \chi}{r_1 r_2 r_3} \left(\frac{r_3^2 r_3^2}{3} - \frac{r_1^2 r_3^2}{2} - \frac{r_1^2 r_2^2}{1} \right). \end{cases} \tag{24}$$

The integral H_2 of the normal form equations becomes:

$$9r_1^2 + 4r_2^2 + r_3^2 = 2E_0, \tag{25}$$

with E_0 a positive (energy) constant. The combination angle $2\phi_3 - \phi_2$ is missing; another integral of the normal form (24) is:

$$2r_2^2 - r_3^2 = C \quad (\text{constant}). \tag{26}$$

In the original variables this integral is:

$$2x_2^2 + \frac{1}{2} \dot{x}_2^2 - x_3^2 - \dot{x}_3^2 = \text{constant}.$$

As we have three independent integrals of the normal form equations (24), the normal form is integrable. Because of the approximative character of the normal form, this means that chaotic motion in the original system (20) is restricted to $O(\varepsilon)$.

Periodic solutions in general position of system (24) exist if $\sin \chi = 0, t \geq 0$ for certain values of the r_i . From the 4th equation of system (24) we find the requirement:

$$\frac{r_2^2 r_3^2}{3} - \frac{r_1^2 r_3^2}{2} - \frac{r_1^2 r_2^2}{1} = 0.$$

Eliminating r_1 by the H_2 integral we find after some rearrangements the condition

$$2r_2^2 r_3^2 + \frac{4}{3} r_2^4 + \frac{1}{6} r_3^4 = \frac{1}{3} E_0 (2r_2^2 + r_3^2), \quad 0 < r_2 < \sqrt{\frac{E_0}{2}}, \quad 0 < r_3 < \sqrt{2E_0}. \tag{27}$$

Both for $\chi = 0$ and for $\chi = \pi$ we find from condition (27) tori imbedded in the energy manifold. The two tori consist of periodic solutions in general position connecting the x_2 and x_3 normal modes. Their period is $O(\varepsilon)$ modulated by their position on the tori. The relation between the presence of a continuous family of periodic solutions on the energy manifold and the existence of another integral (26) is an example of a more general theory on characteristic exponents of periodic solutions developed by Poincaré in [11, vol. 1].

Periodic Solutions in the Coordinate Planes It is clear from the intermediate normal form (22) that the normalized equations of motion will contain all three normal modes. We will use co-moving coordinates $(y_1, y_2, z_1, z_2, u_1, u_2)$ to normalize and to study the stability:

$$\begin{cases} x_1 = y_1 \cos 3t + \frac{1}{3} y_2 \sin 3t, & \dot{x}_1 = -3y_1 \sin 3t + y_2 \cos 3t, \\ x_2 = z_1 \cos 2t + \frac{1}{2} z_2 \sin 2t, & \dot{x}_2 = -2z_1 \sin 2t + z_2 \cos 2t, \\ x_3 = u_1 \cos t + u_2 \sin t, & \dot{x}_3 = -u_1 \sin t + u_2 \cos t. \end{cases} \tag{28}$$

The normalized variables are obtained by averaging over time t and are satisfying the system:

$$\begin{cases} \dot{y}_1 = \varepsilon \frac{7}{6} d_6 (z_1 u_2 + \frac{1}{2} z_2 u_1), \\ \dot{y}_2 = -\varepsilon \frac{7}{2} d_6 (z_1 u_1 - \frac{1}{2} z_2 u_2), \\ \dot{z}_1 = \varepsilon \frac{7}{4} d_6 (-y_1 u_2 + \frac{1}{3} y_2 u_1), \\ \dot{z}_2 = -\varepsilon \frac{7}{2} d_6 (y_1 u_1 + \frac{1}{3} y_2 u_2), \\ \dot{u}_1 = \varepsilon \frac{7}{2} d_6 (-\frac{1}{2} y_1 z_2 + \frac{1}{3} y_2 z_1), \\ \dot{u}_2 = -\varepsilon \frac{7}{2} d_6 (y_1 z_1 + \frac{1}{6} y_2 z_2). \end{cases} \tag{29}$$

The generic picture for the existence of short-periodic solutions in the Hamiltonian 1 : 2 : 3 resonance is given in [10]. As stated above we recover three normal modes instead of generically two; this is caused by the already mentioned degenerate form of Hamiltonian (19).

The three normal modes of the normalized system are harmonic functions:

$$A \cos mt + B \sin mt, \quad m = 3, 2, 1, \quad A^2 + B^2 > 0.$$

To study their stability we linearize around the three normal modes of system (22) to obtain coupled Mathieu-equations; we approximate the characteristic exponents by normalizing the coupled systems. We find in these three cases after some calculations:

1. Normal mode x_1 : put $x_1 = A \cos 3t + B \sin 3t + w_1, x_2 = w_2, x_3 = w_3$.
Transforming in the linearized system by (28) and normalization we find:

$$\begin{aligned} \dot{z}_1 &= -\varepsilon \frac{7}{4} d_6 (B u_1 - A u_2), \\ \dot{z}_2 &= \varepsilon \frac{7}{2} d_6 (A u_1 + B u_2), \\ \dot{u}_1 &= -\varepsilon \frac{7}{2} d_6 \left(B z_1 - \frac{1}{2} A z_2 \right), \\ \dot{u}_2 &= \varepsilon \frac{7}{2} d_6 \left(A z_1 + \frac{1}{2} B z_2 \right). \end{aligned}$$

The eigenvalues of the matrix describing this linear system have multiplicity 2 and are multiples of:

$$\pm \sqrt{A^2 + B^2}.$$

In the nomenclature of [14, Sect. 10.7.3] this is the unstable case HH.

It is interesting to consider the action-simplex with a number of initial conditions near the x_1 normal mode, see Fig. 4. The unstable manifold of the normal mode is two-dimensional but the solutions, displayed by dots in the simplex, remain in a narrow strip extending to the edge where $x_1 = 0$. This is caused by the third integral (26) of the normal form which tells us that the action corresponding with x_1 is proportional to the action of x_2 .

2. Normal mode x_2 : put $x_1 = w_1, x_2 = A \cos 2t + B \sin 2t + w_2, x_3 = w_3$.

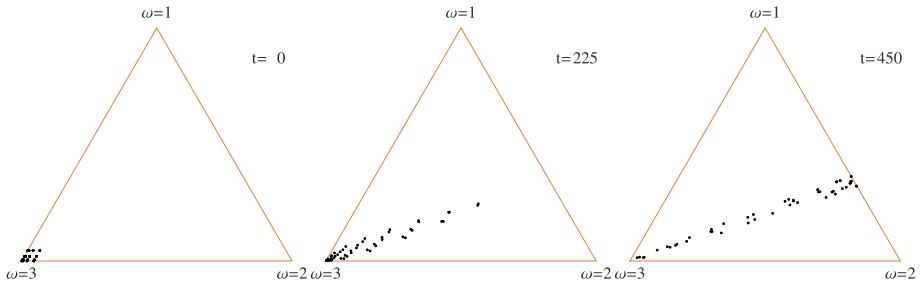


Fig. 4 The $\omega = 3$ normal mode (x_1) exists in the case 0 and is unstable (see also Fig. 6). We consider the time evolution of 98 initial positions near this normal mode by displaying the actions in the action-simplex at $t = 0, 225, 450$. The evolution is based on Hamiltonian (19); $\varepsilon = 0.2$. The unstable manifold is two-dimensional after which the action points remain near a line in the action simplex. The inclination is explained by the expression of the third integral (26) of the normal form

Transforming in the linearized system by (28) and normalization by averaging we find:

$$\begin{aligned} \dot{y}_1 &= -\varepsilon \frac{7}{6} d_6 (B u_1 + A u_2), \\ \dot{y}_2 &= \varepsilon \frac{7}{2} d_6 (A u_1 - B u_2), \\ \dot{u}_1 &= \varepsilon \frac{7}{2} d_6 \left(B y_1 - \frac{1}{3} A y_2 \right), \\ \dot{u}_2 &= \varepsilon \frac{7}{2} d_6 \left(A y_1 + \frac{1}{3} B y_2 \right). \end{aligned}$$

The eigenvalues have multiplicity 2 and are multiples of:

$$\pm i \sqrt{A^2 + B^2}.$$

In the nomenclature of [14] this is the spectrally stable case EE, but with both positive and negative imaginary eigenvalues coincident. A numerical calculation confirms the stability in the sense that the solutions remain near the normal mode during a finite time.

When varying u , this will produce a Hamiltonian-Hopf bifurcation, see the next subsection.

As the normal mode is spectrally stable, it is of interest to display the behaviour of the actions of solutions starting near this normal mode. In Fig. 5 we show that for a limited time interval, the actions stay nearby.

3. Normal mode x_3 : put $x_1 = w_1, x_2 = w_2, x_3 = A \cos t + B \sin t + w_3$.

Transforming in the linearized system by (28) and normalization we find:

$$\begin{aligned} \dot{y}_1 &= -\varepsilon \frac{7}{6} d_6 \left(B z_1 + \frac{1}{2} A z_2 \right), \\ \dot{y}_2 &= \varepsilon \frac{7}{2} d_6 \left(A z_1 - \frac{1}{2} B z_2 \right), \end{aligned}$$

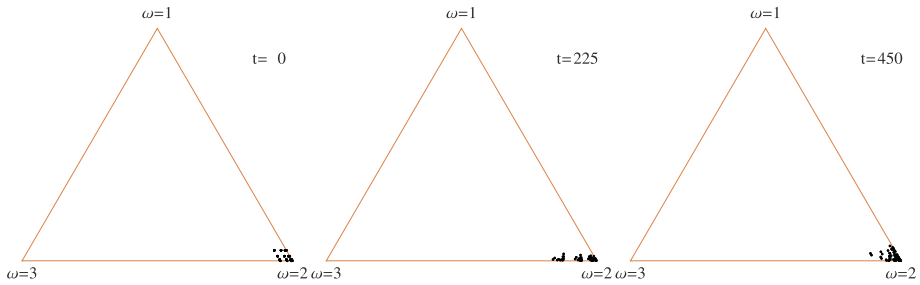


Fig. 5 The $\omega = 2$ normal mode (x_2) is stable in the case 0. We consider the time evolution based on Hamiltonian (19) of 98 initial positions near this normal mode by displaying the actions in the action-simplex at $t = 0, 225, 450$; $\varepsilon = 0.2$

$$\begin{aligned} \dot{z}_1 &= \varepsilon \frac{7}{4} d_6 \left(B y_1 - \frac{1}{3} A y_2 \right), \\ \dot{z}_2 &= \varepsilon \frac{7}{2} d_6 \left(A y_1 + \frac{1}{3} B y_2 \right). \end{aligned}$$

The eigenvalues have multiplicity 2 and are multiples of:

$$\pm i \sqrt{A^2 + B^2}.$$

In the nomenclature of [14, Sect. 10.7.3] this is the spectrally stable case EE, but again with both positive and negative imaginary eigenvalues coincident. The numerical behaviour (not shown) looks similar to Fig. 5.

Our choice of well-balanced masses involves the symmetry $a_1 = a_3$. In the sequel we will see that other choices of masses producing 1 : 2 : 3 resonance give qualitatively different results. It is interesting to compare the dynamics of case 0 ($u = d_9 = 0$) with the dynamics for $u > 0$. Such a comparison will be given in the next subsections.

4.2 The Hamiltonian-Hopf Bifurcation

In the preceding subsection we considered a rather symmetric case, $a_1 = a_3$, corresponding with $u = 0$, producing an integrable normal form; see Sect. 3.6 and Table 2. We will now consider the cases $0 < u < u_1 (= 0.887732\dots)$; as u increases through the interval $(0, u_1)$ the masses will differ more and more, producing generic Hamiltonians. To put system (16) in the standard form of perturbed harmonic equations we have to apply again a symplectic transformation, i.e. (12) from Sect. 3.6. This leads to a transformed Hamiltonian (with rescaled frequencies) of the form $H_2 + \varepsilon H_3$ with

$$H_2 = \frac{1}{2} \left(\dot{x}_1^2 + \frac{9}{14} x_1^2 + \dot{x}_2^2 + \frac{4}{14} x_2^2 + \dot{x}_3^2 + \frac{1}{14} x_3^2 \right)$$

and

$$\left\{ \begin{aligned} H_3 &= d_1 x_1^3 + d_2 x_2 x_1^2 + d_3 x_3 x_1^2 + d_4 x_2^2 x_1 + d_5 x_3^2 x_1 + d_6 x_1 x_2 x_3 + d_7 x_2^3 + d_8 x_3^3 \\ &\quad + d_9 x_2 x_3^2 + d_{10} x_2^2 x_3, \end{aligned} \right. \tag{30}$$

with all coefficients non-zero, see Table 2. After rescaling time $t \rightarrow t/\sqrt{14}$, the equations of motion for the three dof system can be written as:

$$\begin{cases} \ddot{x}_1 + 9x_1 = -\varepsilon 14(3d_1x_1^2 + 2d_2x_1x_2 + 2d_3x_1x_3 + d_4x_2^2 + d_5x_3^2 + d_6x_2x_3), \\ \ddot{x}_2 + 4x_2 = -\varepsilon 14(d_2x_1^2 + 2d_4x_2x_1 + d_6x_1x_3 + 3d_7x_2^2 + d_9x_3^2 + 2d_{10}x_2x_3), \\ \ddot{x}_3 + x_3 = -\varepsilon 14(d_3x_1^2 + 2d_5x_3x_1 + d_6x_1x_2 + 3d_8x_3^2 + 2d_9x_2x_3 + d_{10}x_2^2). \end{cases} \tag{31}$$

The size of the coefficients of H_3 are comparable with the size of d_6 or smaller, we will give them explicitly as examples for the cases 1 and 2 in Sect. 4.3 with less balanced masses.

In the cubic part of the normalized Hamiltonian we retain of the cubic part only the terms with d_6 and d_9 ; the other terms are, after normalization, active only at higher order. So, anticipating this, an intermediate normal form of the equations of motion becomes:

$$\begin{cases} \ddot{x}_1 + 9x_1 = -\varepsilon 14d_6x_2x_3, \\ \ddot{x}_2 + 4x_2 = -\varepsilon 14(d_6x_1x_3 + d_9x_3^2), \\ \ddot{x}_3 + x_3 = -\varepsilon 14(d_6x_1x_2 + 2d_9x_2x_3), \end{cases} \tag{32}$$

The Normal Form and Periodic Solutions Outside the Coordinate Planes Using transformation (23) and putting $\phi_1 - \phi_2 - \phi_3 = \chi_1$, $2\phi_3 - \phi_2 = \chi_2$, we find after averaging-normalization:

$$\begin{cases} \dot{r}_1 = \varepsilon \frac{7}{6} d_6 r_2 r_3 \sin \chi_1, \\ \dot{r}_2 = -\varepsilon \frac{7}{4} (d_6 r_1 r_3 \sin \chi_1 + d_9 r_3^2 \sin \chi_2), \\ \dot{r}_3 = -\varepsilon \frac{7}{2} (d_6 r_1 r_2 \sin \chi_1 - 2d_9 r_2 r_3 \sin \chi_2), \\ \dot{\chi}_1 = \varepsilon \frac{7}{2} [d_6 \frac{\cos \chi_1}{r_1 r_2 r_3} (\frac{r_2^2 r_3^2}{3} - \frac{r_1^2 r_3^2}{2} - \frac{r_1^2 r_2^2}{1}) - d_9 \frac{\cos \chi_2}{r_2} (\frac{1}{2} r_3^2 + 2r_2^2)], \\ \dot{\chi}_2 = \varepsilon \frac{7}{4} (d_6 \frac{r_1 \cos \chi_1}{r_2 r_3} (4r_2^2 - r_3^2) + d_9 \frac{\cos \chi_2}{r_2} (8r_2^2 - r_3^2)). \end{cases} \tag{33}$$

The integral H_2 of the normal form equations becomes again:

$$9r_1^2 + 4r_2^2 + r_3^2 = 2E_0, \tag{34}$$

Periodic solutions in general position with constant amplitude have to satisfy $\sin \chi_1 = \sin \chi_2 = 0$ or $\chi_1 = 0, \pi$ and $\chi_2 = 0, \pi$. We have

$$\cos \chi_1 \cos \chi_2 = \pm 1, \quad q = \frac{d_9}{d_6} > 0.$$

From the last two equations of system (33) we have the conditions:

$$\frac{r_2^2 r_3^2}{3} - \frac{r_1^2 r_3^2}{2} - \frac{r_1^2 r_2^2}{1} = \pm q r_1 r_3 \left(\frac{1}{2} r_3^2 + 2r_2^2 \right), \tag{35}$$

$$4r_2^2 - r_3^2 = \pm q \frac{r_3}{r_1} (r_3^2 - 8r_2^2). \tag{36}$$

Eliminating r_1 from (35) using (36) we obtain two equations that are quadratic in r_2^2 and r_3^2 . Eliminating r_1 from the H_2 integral we find one equation that is quadratic in r_2^2 and r_3^2 .

These expressions have to be handled for the range of q determined by $u \in (0, u_1)$. Using MATHEMATICA and corresponding plots we find four positive solutions corresponding with four periodic solutions characterized by two different phases.

We omit the stability analysis, but note that the generic case of the 1 : 2 : 3 resonance was studied in [10] that produces four general position periodic solutions with the stability types EE and EH .

Periodic Solutions in the Coordinate Planes Inspection of the intermediate normal form system (32) shows that the x_1 and x_2 normal modes exist as solutions of this system, the x_3 normal mode does not. It is shown in [10] that the normal mode x_2 is unstable. If the instability is of class C (complex eigenvalues), a Shilnikov-Devaney bifurcation [6] may take place resulting in chaotic dynamics originating from a neighbourhood of the complex unstable normal mode. To avoid singularities near the normal modes we use again the co-moving variables from transformation (28). The normalized variables satisfy the system:

$$\begin{cases} \dot{y}_1 = \varepsilon^7 d_6(z_1 u_2 + \frac{1}{2} z_2 u_1), \\ \dot{y}_2 = -\varepsilon^7 d_6(z_1 u_1 - \frac{1}{2} z_2 u_2), \\ \dot{z}_1 = \varepsilon^7 [\frac{1}{2} d_6(-y_1 u_2 + \frac{1}{3} y_2 u_1) + d_9 u_1 u_2], \\ \dot{z}_2 = -\varepsilon^7 [d_6(y_1 u_1 + \frac{1}{3} y_2 u_2) + d_9(u_1^2 - u_2^2)], \\ \dot{u}_1 = \varepsilon^7 [d_6(-\frac{1}{2} y_1 z_2 + \frac{1}{3} y_2 z_1) + d_9(-2z_1 u_2 + z_2 u_1)], \\ \dot{u}_2 = -\varepsilon^7 [d_6(y_1 z_1 + \frac{1}{6} y_2 z_2) + d_9(2z_1 u_1 + z_2 u_2)]. \end{cases} \tag{37}$$

We find three families of short-periodic solutions; the constants A, B are real, $A^2 + B^2 > 0$.

1. $x_1(t) = A \cos 3t + B \sin 3t, x_2 = x_3 = 0$.
2. $x_2(t) = A \cos 2t + B \sin 2t, x_1 = x_3 = 0$.
3. If $x_2(t) = 0, d_6 \neq 0$:

$$\begin{cases} x_1(t) = \frac{d_9}{d_6} (\frac{A}{A^2+B^2} (3B^2 - A^2) \cos 3t - \frac{B}{A^2+B^2} (3A^2 - B^2) \sin 3t), \\ x_3(t) = A \cos t + B \sin t. \end{cases} \tag{38}$$

If d_9 differs from zero, this family of periodic solutions moves along the $x_2 = 0$ edge of the simplex in Fig. 6 starting from the x_3 normal mode that exists if $d_9 = 0$.

To evaluate the stability of the periodic solutions we will linearize system (32) near these solutions; this produces coupled Mathieu equations which we will analyze by normalization.

The x_2 Normal Mode Put:

$$x_1 = w_1, \quad x_2 = A \cos 2t + B \sin 2t + w_2, \quad x_3 = w_3,$$

with real constants $A, B, A^2 + B^2 > 0$ and corresponding expressions for the derivatives. We find after linearization

$$\begin{cases} \ddot{w}_1 + 9w_1 = -\varepsilon 14d_6(A \cos 2t + B \sin 2t)w_3, \\ \ddot{w}_2 + 4w_2 = 0, \\ \ddot{w}_3 + w_3 = -\varepsilon 14[d_6 w_1(A \cos 2t + B \sin 2t) + 2d_9(A \cos 2t + B \sin 2t)w_3], \end{cases} \tag{39}$$

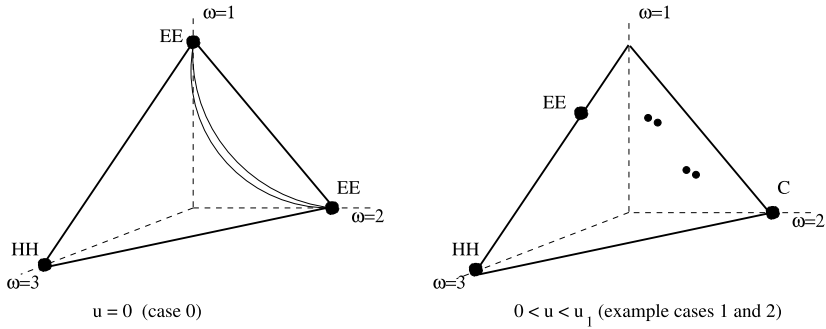


Fig. 6 The action simplices of the cases $u = 0$ and $0 < u < u_1$; the cases 1 and 2 are typical for the family of Hamiltonians where $u \neq 0$. The actions τ_i (related to r_i^2) form a triangle for fixed values of H_2 which is an integral of the normal forms. The frequencies have been normalized to 1, 2, 3 to indicate the x_3, x_2, x_1 normal mode positions at the vertices. The *black dots* indicate periodic solutions, the indicated stability types are HH (hyperbolic-hyperbolic), EE (elliptic-elliptic) and C (complex). The *two (roughly sketched) curves* connecting the x_2 and x_3 normal modes in the left simplex correspond with two tori consisting of periodic solutions, respectively with combination angles $\chi = 0$ and π . The tori break up into 4 general position periodic solutions if $u > 0$ (cases 1 and 2)

We study the stability of this system by normalization to find the eigenvalues of the matrix (omitting the factor $7\varepsilon/2$)

$$\begin{pmatrix} 0 & 0 & \frac{d_6}{3} B & \frac{d_6}{3} A \\ 0 & 0 & -d_6 A & d_6 B \\ -d_6 B & \frac{d_6}{3} A & 2d_9 B & -2d_9 A \\ -d_6 A & -\frac{d_6}{3} B & -2d_9 A & -2d_9 B \end{pmatrix}$$

produce first order approximations of the characteristic exponents of system (39). For the eigenvalues we find apart from the factor $7\varepsilon/2$:

$$\lambda^2 = -(A^2 + B^2) \left[\left(\frac{1}{3}d_6^2 - 2d_9^2 \right) \pm 2d_9 \sqrt{d_9^2 - \frac{1}{3}d_6^2} \right].$$

A sufficient condition for the complex case C to arise is

$$d_6^2 > 6d_9^2. \tag{40}$$

This condition corresponds with the condition in Table 1 of [10]. Condition (40) is satisfied for $0 < u < u_1$ so that the complex case C arises for $u > 0$.

Another view of the eigenvalues is obtained by realizing that in Sect. 4.1 we had $u = 0$ resulting in $d_6 \neq 0, d_9 = 0$; $u = 0$ gives for the x_2 normal mode purely imaginary eigenvalues with multiplicity two. As u increases ($d_9 \neq 0$), the eigenvalues move from the imaginary axis into the complex domain. This is part of the Hamiltonian-Hopf bifurcation, see Fig. 7.

For case 2 (see Sect. 4.3) we show in the action-simplex of Fig. 8 the behaviour of solutions starting near this complex unstable normal mode.

The x_1 Normal Mode For $d_9 = 0$ we have found in the preceding subsection the case HH. This is a generic case of eigenvalues, so for d_9 small enough and $u \in (0, u_1)$ the nature of

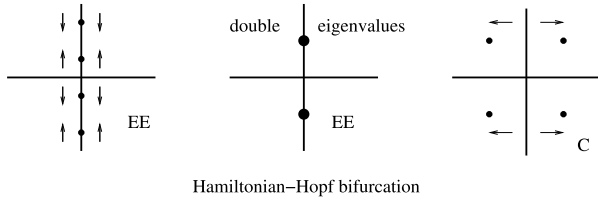


Fig. 7 The Hamiltonian-Hopf bifurcation of a periodic solution in a three dof system as takes place for the x_2 normal mode in $1 : 2 : 3$ resonance of [10]. In our problem we have only the transition from the case of double imaginary eigenvalues to complex eigenvalues as the double eigenvalues are generated by the symmetry at the start of the interval $0 < u < u_1$

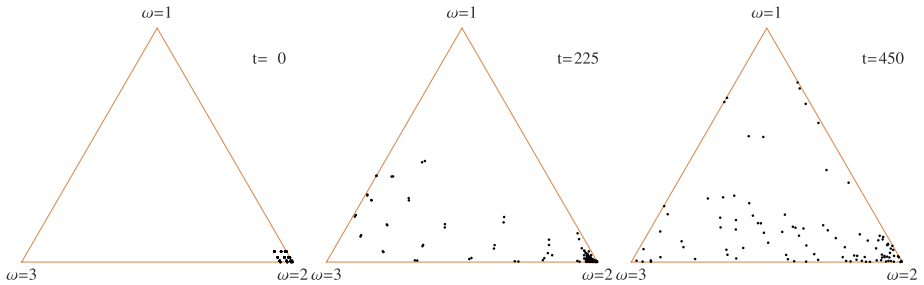


Fig. 8 The $\omega = 2$ normal mode (x_2) exists in the case 2 and is complex unstable (see also Fig. 6). We consider the time evolution of 98 initial positions near this normal mode by displaying the actions in the action-simplex at $t = 0, 225, 450; \epsilon = 0.2$

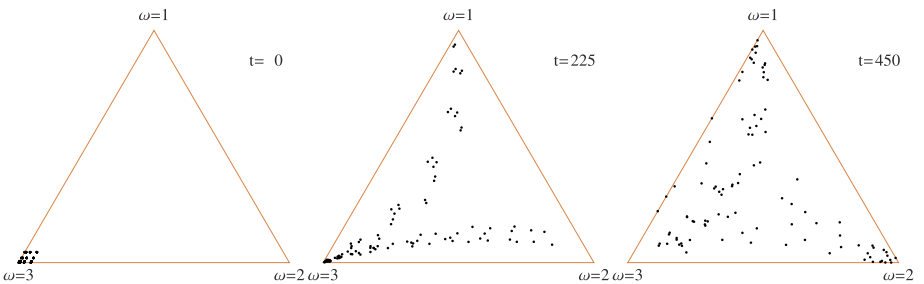


Fig. 9 The $\omega = 3$ normal mode (x_1) exists in the case 2 and is unstable (see also Fig. 6). We consider the time evolution of 98 initial positions near this normal mode by displaying the actions in the action-simplex at $t = 0, 225, 450, \epsilon = 0.2$. The behaviour is different from the case 0, see Fig. 4, as in this case the normal form is not integrable

the instability will not change but the dynamics is very different as the normal form is not integrable.

For case 2 (see Sect. 4.3) we show in the action-simplex of Fig. 9 the behaviour of solutions starting near this unstable normal mode.

The Periodic Solution for $x_2(t) = 0$ For the periodic solution (38) we put:

$$x_1 = C \cos 3t + D \sin 3t, \quad x_3 = A \cos t + B \sin t.$$

Transforming

$$x_1 = C \cos 3t + D \sin 3t + w_1, \quad x_2 = w_2, \quad x_3 = A \cos t + B \sin t + w_3,$$

and substitution into system (32), we find after linearization:

$$\begin{cases} \ddot{w}_1 + 9w_1 = -\varepsilon 14d_6(A \cos t + B \sin t)w_2, \\ \ddot{w}_2 + 4w_2 = -\varepsilon 14[d_6(C \cos 3t + D \sin 3t)w_1 + d_6(A \cos t + B \sin t)w_1 \\ \quad + 2d_9(A \cos t + B \sin t)w_3], \\ \ddot{w}_3 + w_3 = -\varepsilon 14[d_6(C \cos 3t + D \sin 3t)w_2 + 2d_9(A \cos t + B \sin t)w_2]. \end{cases} \tag{41}$$

To investigate stability we normalize near the periodic solution; apart from a factor $7\varepsilon/2$, this produces the matrix:

$$\begin{pmatrix} 0 & 0 & \frac{d_6}{3}B & \frac{d_6}{6}A & 0 & 0 \\ 0 & 0 & -d_6A & \frac{d_6}{2}B & 0 & 0 \\ -\frac{d_6}{2}B & \frac{d_6}{6}A & 0 & 0 & d_6\frac{D}{2} + d_9B & -d_6\frac{C}{2} + d_9A \\ -d_6A & -\frac{d_6}{3}B & 0 & 0 & -d_6C - 2d_9A & -d_6D + 2d_9B \\ 0 & 0 & d_6D - 2d_9B & -d_6\frac{C}{2} + d_9A & 0 & 0 \\ 0 & 0 & -d_6C - 2d_9A & -d_6\frac{D}{2} - d_9B & 0 & 0 \end{pmatrix}.$$

Using the values of C and D given in (38), we find purely imaginary eigenvalues with multiplicity two. The results have been summarized in Fig. 6.

4.3 Experiments for Two Cases with $u > 0$

The first order normal form of system (31) produces qualitatively the same dynamics for $u \in (0, u_1)$. We consider a few experiments for two cases that are typical for this dynamics.

Case 1 with Less-Balanced Masses We choose for $u = 0.534105$ from Eqs. (9)):

$$a_1 = 0.00510292, \quad a_2 = 0.117265, \quad a_3 = 0.0854008, \quad a_4 = 0.292231$$

In this case we have $m_1 > m_3 > m_2 > m_4$. With these mass (a_i) values the symplectic transformation of Sect. 3.6 to system (31) produces the expression:

$$\begin{aligned} H_3 = & 0.0281999x_1^3 - 0.0258437x_1^2x_2 - 0.0777574x_1^2x_3 - 0.0275058x_1x_2^2 \\ & - 0.00252349x_1x_3^2 - 0.0306229x_1x_2x_3 + 0.0157538x_2^3 + 0.000502655x_3^3 \\ & - 0.0089438x_2x_3^2 + 0.028527x_2^2x_3. \end{aligned}$$

We have the case:

$$d_6 = -0.0306229, \quad d_9 = -0.0089438.$$

so that the x_2 normal mode is complex unstable; see Fig. 6. The $H_2(t)$ time series are shown in Fig. 10.

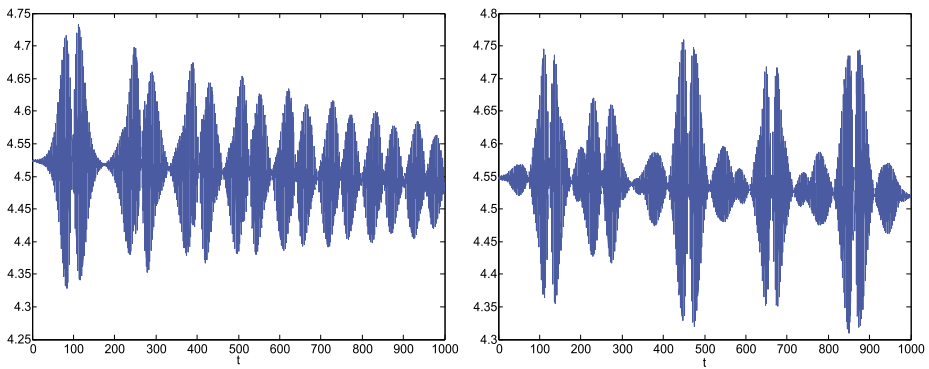


Fig. 10 The $H_2(t)$ time series (sum of the actions) based on system(32) of case 1 for two sets of initial values. (Left) Starting near the x_1 normal mode plane with $x_1 = 1, x_2 = 0.1, x_3 = 0.1, \dot{x}_i = 0, i = 1, 2, 3; \varepsilon = 0.5, H_2(0) \approx 4.52$. The variations of H_2 start with 0.4 and are near $t = 1000$ 0.15. Energy is pumped into H_3 . (Right) The $H_2(t)$ time series starting near the complex unstable normal mode x_2 with $x_1 = 0.1, x_2 = 1.5, x_3 = 0.1, \dot{x}_i = 0, i = 1, 2, 3; \varepsilon = 0.5, H_2(0) \approx 4.52$. The variations of H_2 are 0.4. Horizontal scales: time in $[0, 1000]$, vertical scales: H_2 in $[4.25, 4.75]$

Note that d_θ is still fairly small with the implication that the expansion of the flow near the x_2 normal mode will not be very explosive. This may reduce the amount of chaos present in the system. We compare with case 0 and give a few more details for different initial conditions based on integration of system (22) and system (32). We established that in all cases the x_1 normal mode is unstable (HH), see also Fig. 6. Starting near the x_1 normal mode in case 0, the solutions move away, guided by the two-dimensional unstable manifold of the normal mode; the integrability of the normal form produces a fairly regular $H_2(t)$ with variations 0.05. In Fig. 10 we display $H_2(t)$ for case 1 with the same initial conditions showing strong variations of $H_2(t)$; its behaviour is influenced by the chaotic character of the normal form. On this interval of time $[0, 1000]$, energy is clearly pumped into H_3 but the recurrence of the Hamiltonian system will return this on a much longer timescale.

The chaos in case 1 (and 2) is strongly influenced by the complex instability of the x_2 normal mode. In case 0 this mode is stable so that $H_2(t)$ varies again with 0.05 only. Using the same initial conditions for case 1 we find strong variations (0.4) of $H_2(t)$, but always within the limits of the error estimates; see Fig. 10, right.

Case 2 with Less-Balanced Masses We choose for $u = 0.826713$ from Eqs. (9) a case with even less balanced masses; in this case m_1 is quite massive. We have:

$$a_1 = 0.000685158, \quad a_2 = 0.11239, \quad a_3 = 0.100269, \quad a_4 = 0.286656.$$

With these mass (a_i) values the symplectic transformation of Sect. 3.6 to system (31) produces the expression:

$$\begin{aligned} H_3 = & 0.0352657x_1^3 - 0.0272316x_1^2x_2 - 0.0743155x_1^2x_3 - 0.0366184x_1x_2^2 \\ & - 0.00260064x_1x_3^2 - 0.0337877x_1x_2x_3 + 0.0181144x_2^3 + 0.000760425x_3^3 \\ & - 0.0105601x_2x_3^2 + 0.023904x_2^2x_3. \end{aligned}$$

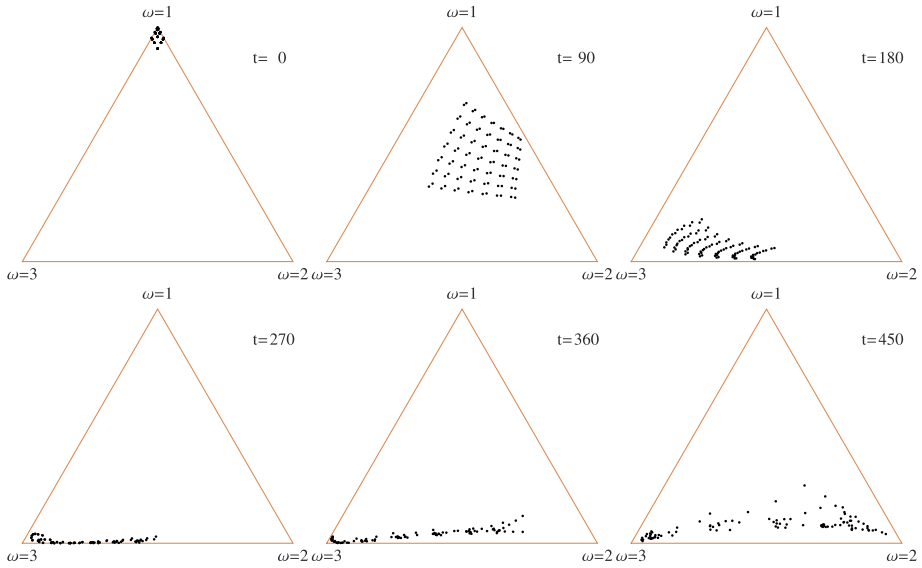


Fig. 11 We consider for case 2 the time evolution of 98 starting points near the $\omega = 1$ vertex by displaying the action-simplex at various times

We have the case:

$$d_6 = -0.0337877, \quad d_9 = -0.0105601$$

If $d_9 \neq 0$ (the cases 1 and 2), the x_3 normal mode does not exist. In Fig. 11 we show the action-simplex for solutions starting near the $x_1 = x_2 = 0$ position, so near the $\omega = 1$ vertex.

We computed the $H_2(t)$ time series of case 2 based on system (32); we omit the picture as it is similar to Fig. 10, right.

4.4 Comparison with Another Hamiltonian System in 1 : 2 : 3 Resonance

It is instructive to discuss our results for the inhomogeneous FPU chain with another Hamiltonian system in 1 : 2 : 3 resonance, and compare the instability types of the x_2 normal mode. In this system we have a full Hamiltonian-Hopf bifurcation as sketched in Fig. 7.

For the inhomogeneous FPU lattice in 1 : 2 : 3 resonance we found complex instability (C) of the x_2 normal mode and no cases of HH instability. Both cases, HH and C lead to a non-integrable normal form but the dynamics is different. See [5].

To illustrate the different dynamics consider the Hamiltonian presented as an example in [18]:

$$H(p, q) = \frac{1}{2}(p_1^2 + q_1^2) + (p_2^2 + q_2^2) + \frac{3}{2}(p_3^2 + q_3^2) - \varepsilon q_1^2(a_2 q_2 + a_3 q_3) - \varepsilon b q_1 q_2 q_3. \quad (42)$$

This system is in 1 : 2 : 3 resonance but it is not derived from a FPU chain. We present $H_2(t)$ for both instability cases in Fig. 12. The dynamics is chaotic but in the case left, the q_2 normal mode is unstable with real eigenvalues (HH); transverse homoclinic intersections produce chaotic motion. On the right the q_2 normal mode is complex unstable (C) which

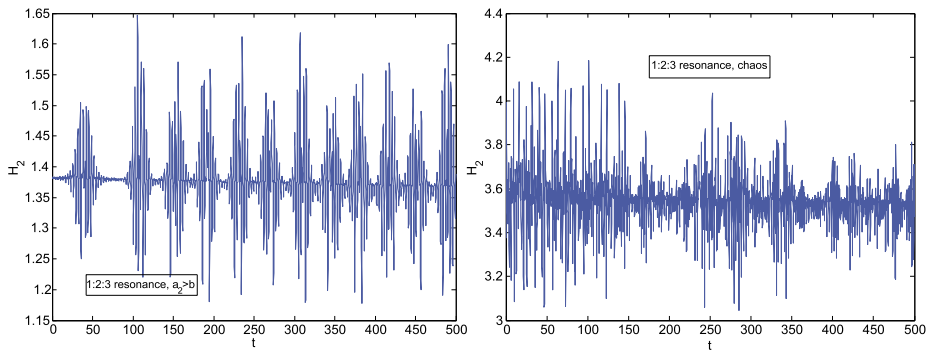


Fig. 12 Two $H_2(t)$ time series based on Hamiltonian (42). On the *left* $x_1(0) = 0.1$, $x_2(0) = 1$, $x_3(0) = 0.5$, and on the *right* $x_1(0) = 2$, $x_2(0) = 1$, $x_3(0) = -0.05$. For both time series we use $\varepsilon = 0.5$, $a_2 = 3$, $a_3 = 1$, $b = 1$, and $\dot{x}_1(0) = \dot{x}_2(0) = \dot{x}_3(0) = 0$. For the x_2 normal mode we have instability HH on the *left* and instability C on the *right*. In both cases the Hamiltonian flow is chaotic but in the right picture the system has undergone Devaney-Shilnikov bifurcation. *Horizontal scales*: time in $[0, 500]$, *vertical scales*: energy in $[1.15, 1.65]$ (*left*) and in $[3, 4.5]$ (*right*)

produces the Hamiltonian Devaney-Shilnikov phenomenon. This involves a homoclinic orbit surrounded by an infinite number of unstable periodic solutions producing more violent chaotic motion as predicted in [6].

5 Conclusions

General

- For an inhomogeneous periodic FPU-chain with four particles, most frequency ratios occur for a one-dimensional variety of mass ratios. The frequency ratios $1 : 2 : 1$ and $1 : 1 : 3$ arise for a finite number of mass ratios, the ratios $1 : 2 : 2$, $1 : 1 : 1$ and $1 : 3 : 3$ do not occur at all in this FPU-chain. See Table 1.
- For any number of particles $n \geq 3$ the set of mass distributions for a given frequency distribution has a relatively simple algebraic structure. For $n = 4$ we describe algorithmically how to determine this set for a given frequency distribution. For $n \geq 4$ there are frequency distributions that do not correspond to any mass distribution.
- Applications.

There are many applications of chains of particles. A large number focuses on molecular dynamics; in fact normalization was introduced and used in one of the classics on atomic dynamics [1]. A recent result is to construct a chain of FPU cells where each cell is a 4-particles FPU system, weakly connected with identical cells; see [19]. Another application based on normal forms and related symmetry considerations is to consider a chain of $2n$ particles with alternating masses; see [9] and [3].

The Case of Four Particles in $1 : 2 : 3$ Resonance

- The α -chain with four particles in $1 : 2 : 3$ resonance does not contain the case of the second normal mode with HH instability. For nearly all mass ratios it contains the second normal mode with complex C instability showing the generic features of the general $1 : 2 : 3$ resonance described in [10].

In this sense it is very different from the classical FPU system with equal masses where many resonances arise in the spectrum that are not effective, see [13].

- A special case of the resonance $1 : 2 : 3$ has the symmetry of two opposite equal masses and two quite different masses. Along the variety of mass ratios as a limit case one of the masses tends to infinity.
- The symmetric case of two equal masses differs dynamically from the other cases. The transition to four different masses corresponds to half of a Hamiltonian-Hopf bifurcation with a Shilnikov-Devaney bifurcation producing chaotic dynamics. In a more general context such behaviour of the $1 : 2 : 3$ resonance was described in [10].
- The normalized system for the symmetric case of two equal masses is integrable and has periodic solutions for each of the three eigenmodes (the normal modes). Moreover, there are on the energy manifold two families of periodic solutions connecting the second and the third eigenmode. This is a degeneration in the sense described by Poincaré [11, vol. 1]. The symmetry in this special case makes the $1 : 2 : 3$ resonance more similar to the classical FPU problem.
- Under the transition away from the symmetric case, the eigenmodes x_1 (associated with frequency 3) and x_2 (associated with frequency 2) produce a periodic solution (normal mode) in the nonlinear system. The periodic solution that was associated to the third eigenmode in the symmetric case moves away along an edge of the action simplex. The two continuous families of periodic solutions of the symmetric case break up into four periodic solutions.
- To summarize: the inhomogeneous periodic FPU α -chain with four particles is characterized by a non-integrable normal form, except in the symmetric case of two equal masses. The implication is that near stable equilibrium its chaotic behaviour is not restricted to exponentially small sets as in the case of two dof systems and as in the case of the classical FPU α -chain.

Considering Again the Classical FPU Chain

- We have shown that in the case of four particles the presence of two equal masses produces a symmetry in the dynamical system that makes the system structurally unstable. In this perspective the model of the classical FPU chain with all masses equal is also structurally unstable and misleading as a model.
- The averaging-normal form technique we have used is valid for an arbitrary number of particles as long as the total energy of the chain is finite and small. This enables us to extend the analysis to chains with many particles as was shown in [13].
- The dynamics on the energy manifold is structured by approximate invariant manifolds, some of them valid for all time, some with finite but long validity ($1/\varepsilon^m$ intervals for some positive m). At the same time the Poincaré recurrence theorem produces relatively short recurrence times, see [19]. Altogether this suggests that the classical FPU chain for low energy values does not lead to equipartition of energy and is not a good model for statistical mechanics.

Acknowledgements Numerical calculations in this paper were carried out by MATCONT (ode 78) under MATLAB; installation and instructions for use of the software by Taoufik Bakri is gratefully acknowledged.

Open Access This article is distributed under the terms of the Creative Commons Attribution 4.0 International License (<http://creativecommons.org/licenses/by/4.0/>), which permits unrestricted use, distribution, and reproduction in any medium, provided you give appropriate credit to the original author(s) and the source, provide a link to the Creative Commons license, and indicate if changes were made.

Appendix

In Sect. A.1 we discuss a few facts that are valid for any number of particles $n \geq 3$. This enables us to start studying resonances in arbitrary long chains. In Sect. A.2 we give an overview of the relations between frequency ratios and mass ratios valid for all systems with four particles. This might be useful for studying network models as considered in [19]. In Sect. A.3 we discuss some details relevant for the analysis of the 1 : 2 : 3 ratio of frequencies.

A.1 Results for n Particles

Our main general result is the following.

Proposition A.1 *If the number of particles is equal to 3 then each choice of eigenvalues $\lambda_1 \geq \lambda_2 > \lambda_3 = 0$ occurs for some positive diagonal matrix A_3 .*

If $n \geq 4$, there are choices of eigenvalues $\lambda_1 \geq \lambda_2 \geq \dots \geq \lambda_{n-1} > \lambda_n = 0$ for which there are no positive diagonal matrices A_n such that $A_n C_n$ has these eigenvalues.

To show this we use Lemma A.2, which gives the description of the top coefficients in (7), and Proposition A.3, which restricts the fibers to compact sets in \mathbb{R}^n .

Lemma A.2 *The polynomials p_{n-1} and p_{n-2} have the form indicated in (7).*

Proof If we replace the entries -1 at positions $(1, n)$ and $(n, 1)$ in C_n by 0 we obtain the Cartan matrix C_n for the root system of type A_n . (See, e.g., [2, Déf. 3 in 1.5 of Chap. 6, and Planche I].) The determinant of C_n is known to be $n + 1$.

If all a_j are non-zero, the characteristic equation is equivalent to $\det(C_n - \lambda A_n^{-1}) = 0$. We determine first the factor of $(-\lambda)^{n-1}$. In the expansion of the determinant the term with λ at all diagonal positions except at (j, j) is equal to

$$2 \prod_{i \neq j} (-\lambda a_i^{-1}) = 2(-\lambda)^{n-1} a_j / (a_1 a_2 \dots a_n).$$

So the factor of $(-\lambda)^{n-1}$ in $\det(AC_n - \lambda I_n)$ is $\sum_j 2a_j = p_{n-1}(a)$.

For the factor of $(-\lambda)^{n-2}$ we have contributions of two types: Two diagonal positions j and $j + 1$ (modulo n) lead to a contribution of the form $\det(C_2) \prod_{i \neq j, j+1} (-\lambda) / a_i$. Two non-adjointing diagonal positions j_1, j_2 contribute $2 \cdot 2 \sum_{i \neq j_1, j_2} (-\lambda) / a_i$. This leads to the description of $p_{n-2}(a)$. □

By scaling we arrange that the vectors $(\lambda_1, \dots, \lambda_{n-1}, 0)$ of eigenvalues of $A_n C_n$ satisfy $\sum_{j=1}^{n-1} \lambda_j = 1$, and we put $\eta = e_2(\{\lambda_1, \dots, \lambda_{n-1}\})$. Then the points of the fiber of a given vector of eigenvalues are elements of the following set Q_η :

Proposition A.3 *Let $n \geq 3$. For given $\eta > 0$ denote by Q_η the set of points $a \in \mathbb{R}^n$ satisfying*

$$p_{n-2}(a) = \eta, \quad p_{n-1}(a) = 1. \tag{43}$$

Then

- (a) *If $\eta < \frac{1}{2} - \frac{3}{4n}$, then Q_η is a compact quadric in the hyperplane $a_1 + \dots + a_n = \frac{1}{2}$ in \mathbb{R}^n with a non-empty intersection with $\mathbb{R}_{>0}^n$.*

- (b) If $\eta = \frac{1}{2} - \frac{3}{4n}$, then Q_η consists of one point in $\mathbb{R}_{>0}^n$.
- (c) If $\eta > \frac{1}{2} - \frac{3}{4n}$, then $Q_\eta = \emptyset$.

Proof Let $P = C_n - 6I_n + 4E$, with E the $n \times n$ -matrix with all elements equal to 1. Then, considering $a = (a_1, \dots, a_n)$ as a row vector, we have

$$p_{n-2}(a) = \frac{1}{2} a P a^T.$$

There are orthogonal matrices U such that $U^T C_n U = \Lambda$, where Λ is the diagonal matrix with the eigenvalues λ_j of C_n on the diagonal. We put the eigenvalue 0, with eigenvector \mathbf{e} as the last one. Then $\mathbf{e}^T = U(0, \dots, 0, \sqrt{n})^T$, and the last column of U is $\frac{1}{\sqrt{n}} \mathbf{e}^T$. This gives

$$p_{n-1}(a) = 2 \sum_j a_j = 2a \mathbf{e}^T = 2\sqrt{n}(aU)_n, \tag{44}$$

$$p_{n-2}(a) = \frac{1}{2} a (C_n - 6I_n) a^T + 2a E a^T = \frac{1}{2} a U (\Lambda - 6I_n) U^T a^T + \frac{1}{2} (p_{n-1}(a))^2. \tag{45}$$

Because of (44) the points in the hyperplane $p_{n-1}(a) = 1$ can be described as

$$a = \left(x_1, x_2, \dots, x_{n-1}, \frac{1}{2\sqrt{n}} \right) U^T.$$

We write $x = (x_1, \dots, x_{n-1})$. We find the equation

$$\begin{aligned} \eta &= \frac{1}{2} (x, 1/(2\sqrt{n})) (\Lambda - 6I) (x, 1/(2\sqrt{n}))^T + \frac{1}{2} \\ &= - \sum_{j=1}^{n-1} \frac{6 - \lambda_j}{2} x_j^2 + \frac{1}{2} - \frac{3}{4n}. \end{aligned} \tag{46}$$

So the points run through a quadratic set in the hyperplane $p_{n-1}(a) = 1$. The eigenvectors of C_n can be chosen as $(\zeta^k, \zeta^{2k}, \dots, \zeta^{nk})$ with $\zeta = e^{2\pi i/n}$, which leads to eigenvalues $2 - 2 \cos 2\pi k/n \in [0, 4]$. So the $6 - \lambda_j$ are strictly positive. The equation becomes

$$\sum_{j=1}^{n-1} \frac{6 - \lambda_j}{2} x_j^2 = \frac{1}{2} - \frac{3}{4n} - \eta. \tag{47}$$

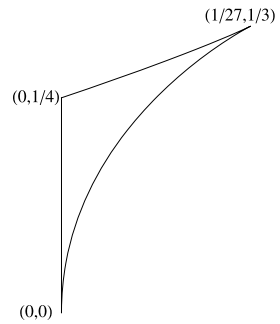
In case (b) in the proposition the single point $x = 0$ corresponds to $\frac{1}{2n} \mathbf{e} \in \mathbb{R}_{>0}^n$. As η decreases the quadric expands in all directions, some of these stay inside $\mathbb{R}_{>0}^n$. □

Proof of Proposition A.1 The choice $\lambda_1 = \dots = \lambda_{n-1} = \frac{1}{n-1}$ leads to

$$\eta = e_2(\{\lambda_1, \dots, \lambda_{n-1}\}) = \binom{n-1}{2} / (n-1)^2 = \frac{1}{2} - \frac{1}{2(n-1)}.$$

This is at most $\frac{1}{2} - \frac{3}{4n}$ if $n = 3$, and strictly larger if $n \geq 4$. Now use Proposition A.3. □

Fig. 13 Region in the ξ - η -plane corresponding to choices of positive eigenvalues. (Horizontal axis: ξ ; vertical axis: η .) The cusp $(\frac{1}{27}, \frac{1}{3})$ is $\Phi(\frac{1}{3}, \frac{1}{3}, \frac{1}{3})$ for Φ as in (50)



A.2 Results for systems consisting of four particles

For $n = 4$ Eqs. (8) determine whether points of the fibers exist. In particular, a (scaled) choice of eigenvalues leads to parameters $\xi, \eta > 0$ which determine the equations for the fiber. We first consider the values of (ξ, η) that can occur:

Proposition A.4 *Let $n = 4$. The set of $(\xi, \eta) = (e_3(\{\lambda_1, \lambda_2, \lambda_3\}), e_2(\{\lambda_1, \lambda_2, \lambda_3\}))$ where $(\lambda_1, \lambda_2, \lambda_3)$ runs through the open triangle in $\mathbb{R}_{>0}^3$ given by $\lambda_1 + \lambda_2 + \lambda_3 = 1$, satisfy*

$$0 < \xi \leq \frac{1}{27}, \quad 0 < \eta \leq \frac{1}{3}, \quad T(\xi, \eta) \leq 0, \tag{48}$$

where

$$T(\xi, \eta) = 27\xi^2 + 4\eta^3 - 18\xi\eta - \eta^2 + 4\xi. \tag{49}$$

Illustration in Fig. 13.

Proof We have to determine the image X of the triangle $T = \{(\lambda_1, \lambda_2, \lambda_3) \in \mathbb{R}_{>0} : \lambda_1 + \lambda_2 + \lambda_3 = 1\}$ under the 6 : 1 map

$$\Phi : (\lambda_1, \lambda_2, \lambda_3) \mapsto (\xi, \eta) = (\lambda_1\lambda_2\lambda_3, \lambda_1\lambda_2 + \lambda_2\lambda_3 + \lambda_3\lambda_1). \tag{50}$$

If a point $(\lambda_1\lambda_2, \lambda_3) \in T$ is mapped to the boundary of the image X , then the derivative matrix of Φ has rank less than 2 at that point. That occurs if two of the coordinates are equal. By S_3 -symmetry it suffices to consider $\lambda_2 = \lambda_3$. The image of the open segment $\{(1 - 2y, y, y) : 0 < y < \frac{1}{2}\}$ consists of the points

$$(\xi, \eta) = (y^2(1 - 2y), y(2 - 3y)).$$

These are points of the curve $T(\xi, \eta) = 0$. They run from $(0, 0)$ to the cusp at $(\frac{1}{27}, \frac{1}{3})$ and then to $(0, \frac{1}{4})$.

The boundary of T consists of three segments, one of them $\{(0, x, 1 - x) : 0 \leq x \leq 1\}$. The image is $\{(0, x(1 - x)) : 0 \leq x \leq 1\}$, the segment from $(\xi, \eta) = (0, 0)$ to $(0, \frac{1}{4})$. By S_3 -invariance the two other boundary segments have the same image.

The image X is the region enclosed by these boundary curves. □

The points (ξ, η) for which the fiber is non-empty form a subset of the region in Proposition A.4. The fiber is empty for $(\frac{1}{27}, \frac{1}{3})$. We give a description of the set of (ξ, η) corresponding to non-empty fibers. We omit the proof. (It can be given along the same lines as

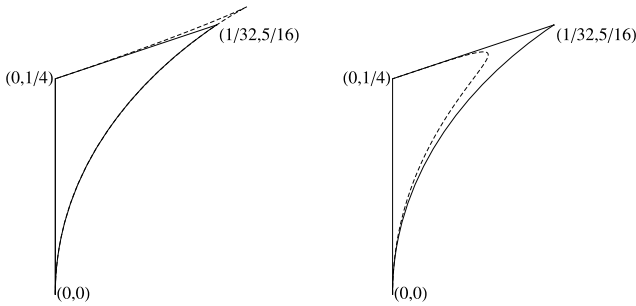


Fig. 14 On the *left* the region in (51) of points (ξ, η) corresponding to non-empty fibers. The *dashed line* gives (part of) the boundary of the larger region in Proposition A.4, corresponding to choices of positive eigenvalues. This shows that most of the possible combinations (ξ, η) correspond to a non-empty fiber. On the *right* is again the region in (51), with the subregion in (52) indicated by the *dashed line*. The *points* strictly to the right of the *dashed line* correspond to compact fibers

that of Proposition A.4, but takes much more work.) Below we give a computational scheme for the determination of the fiber for given eigenvalues $\lambda_1, \lambda_2, \lambda_3$. Following this scheme it becomes clear whether the fiber is empty in any individual case.

Proposition A.5 *The set of points (ξ, η) corresponding to a non-empty fiber is equal to*

$$\left\{ (\xi, \eta) \in \mathbb{R}_{>0}^2 : 0 < \xi \leq \frac{1}{32}, 0 < \eta \leq 2\xi + \frac{1}{4}, T(\xi, \eta) \leq 0 \right\}, \tag{51}$$

with T as defined in (49).

The points (ξ, η) for which the fiber is not compact constitute the subset

$$\left\{ (\xi, \eta) \in \left(0, \frac{1}{32}\right) \times \left(0, \frac{5}{16}\right) : 8\xi^2 + \eta^3 - 5\xi\eta - \frac{1}{4}\eta^2 + \frac{9}{8}\xi \leq 0 \right\}. \tag{52}$$

Illustrations in Fig. 14.

A.2.1 Spherical coordinates on ellipsoid

In the case $n = 4$ we may take the orthogonal matrix in the proof of Proposition A.3 in the form

$$U = \begin{pmatrix} -\frac{1}{2} & 0 & \frac{-1}{\sqrt{2}} & \frac{1}{2} \\ \frac{1}{2} & \frac{-1}{\sqrt{2}} & 0 & \frac{1}{2} \\ -\frac{1}{2} & 0 & \frac{1}{\sqrt{2}} & \frac{1}{2} \\ \frac{1}{2} & \frac{1}{\sqrt{2}} & 0 & \frac{1}{2} \end{pmatrix},$$

corresponding to the eigenvalues 4, 2, 2, 0. This gives

$$\begin{aligned} x_1 &= \frac{-a_1 + a_2 - a_3 + a_4}{2}, & x_2 &= \frac{a_4 - a_2}{\sqrt{2}}, \\ x_3 &= \frac{a_3 - a_1}{\sqrt{2}} \end{aligned} \tag{53}$$

Table 3 Instructions to compute fibers for the case $n = 4$. In these instructions we assume that $\eta \neq 4\xi + \frac{3}{16}$. Otherwise we also have to consider $p_{13} \in (0, \xi)$ and investigate whether this leads to further solutions

<p>(i) For given positive eigenvalues put</p> $\eta = \frac{\lambda_1 \lambda_2 + \lambda_2 \lambda_3 + \lambda_3 \lambda_1}{(\lambda_1 + \lambda_2 + \lambda_3)^2}, \quad \xi = \frac{\lambda_1 \lambda_2 \lambda_3}{(\lambda_1 + \lambda_2 + \lambda_3)^3}.$ <p>(ii) Choose $\eta_2 \in (0, \frac{1}{3}\eta)$ and determine η_1 from $\eta = 4\eta_1 + 3\eta_2$. Determine the subinterval $I_1 \subset (0, \frac{1}{16})$ such that $\eta_1 > 0$ for $\eta_2 \in I_1$.</p> <p>(iii) Compute</p> $s_{13} = \frac{1 - \sqrt{1 - 16\eta_2}}{4}, \quad s_{24} = \frac{1 + \sqrt{1 - 16\eta_2}}{4},$ $p_{13} = \frac{\xi/4 - s_{13}\eta_1}{\sqrt{1 - 16\eta_2}/2}, \quad p_{24} = \eta_1 - p_{13}.$ <p>Determine the subset $I_2 \subset I_1$ such that $p_{13} > 0$ and $p_{24} > 0$ for $\eta_2 \in I_2$.</p> <p>(iv) Compute $d_{13} = s_{13}^2 - 4p_{13}$ and $d_{24} = s_{24}^2 - 4p_{24}$. Determine $I_3 \subset I_2$ such that $d_{13} \geq 0$ and $d_{14} \geq 0$.</p> <p>(v) Compute $a_1, a_3 = \frac{1}{2}(s_{13} \mp \sqrt{d_{13}})$ and $a_2, a_4 = \frac{1}{2}(s_{24} \mp \sqrt{d_{24}})$. Determine the subset $I_4 \subset I_3$ such that $a_j > 0$ for $j = 1, \dots, 4$ for $\eta_2 \in I_4$.</p> <p>(vi) Apply all symmetries in the dihedral group D_4 to the points (a_1, \dots, a_4).</p>
--

Points of the fiber give points on the ellipsoid $x_1^2 + 2x_2^2 + 2x_3^2 = \frac{5}{16} - \eta$ in (46). Then spherical coordinates ψ and ϕ are determined by

$$x_1 = \rho \sin \psi, \quad x_2 = \frac{\rho}{\sqrt{2}} \cos \psi \cos \phi, \quad x_3 = \frac{\rho}{\sqrt{2}} \cos \psi \sin \phi, \tag{54}$$

$$\rho = \sqrt{\frac{5}{16} - \eta} > 0, \quad -\frac{\pi}{2} \leq \psi \leq \frac{\pi}{2}, \quad -\pi \leq \phi \leq \pi.$$

These are the coordinates used in Fig. 3 and in the examples below.

A.2.2 Computation of fibers

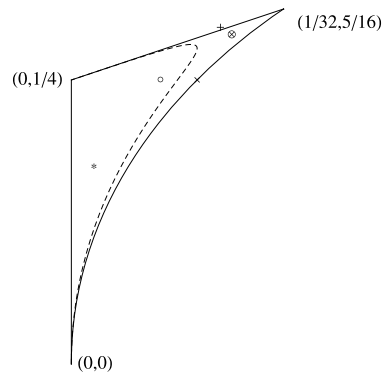
The computation of fibers is guided by the use of the action of the dihedral group D_4 on the solutions. We start with the quantities $\xi, \eta, \eta_1, \eta_2$. These are invariant under the whole group D_4 . (If a point $a = (a_1, a_2, a_3, a_4)$ of the fiber can be found then $\eta_1 = q_1(a)$ and $\eta_2 = q_2(a)$, hence invariant under D_4 .)

The quantity $4(-a_1 + a_2 - a_3 + a_4) = \sqrt{1 - 16\eta_2}$ is invariant under the subgroup $V_4 \subset D_4$ generated by the permutations [1, 3] and [2, 4], and sent to its negative by [1, 2][3, 4]. The group V_4 also leaves invariant the quantities $s_{13} = a_1 + a_3, s_{24} = a_2 + a_4, p_{13} = a_1 a_3,$ and $p_{24} = a_2 a_4$.

In the last stage we determine a_1 and a_3 , invariant under [2, 4] and exchanged by [1, 3]. Similarly a_2 and a_4 are invariant under [1, 3] and exchanged by [2, 4]. The total solution (a_1, a_2, a_3, a_4) is changed by non-trivial elements of D_4 , except in cases with additional symmetry.

In Table 3 the resulting computational scheme is described. It works under the assumption that the point (ξ, η) is not on the line $\eta = 4\xi + \frac{3}{16}$. (This does not happen for the resonances in Table 1.) The parameter u was specially adapted to the resonance 1 : 2 : 3. In general we use $\eta_2 \in (0, \frac{1}{16})$ as the parameter.

Fig. 15 Points corresponding to the resonances 1 : 2 : 3 (○), 1 : 2 : 2 (+), 1 : 1 : 2 (×), 1 : 3 : 6 (*), and 2 : 3 : 4 (⊗)



This approach leads to the resonances in Table 3. We discuss the application to the resonance 1 : 2 : 3, and as an example also to the resonances 1 : 1 : 2, 1 : 3 : 6, and 2 : 3 : 4, which are typical for the different cases in Table 1.

The Resonance 1 : 2 : 3 In this case we used a real parameter u satisfying $\sqrt{1 - 16\eta_2} = \frac{5-u}{7}$. This leads to simpler expressions for the solutions, and for the transformation matrices. Initially, $u \in (-2, 5]$.

In step iii. in Table 3 we find $s_{13} = \frac{2+u}{28}$ and $s_{24} = \frac{12-u}{28}$. The system

$$p_{13} + p_{24} = \eta_1, \quad s_{13}p_{24} + s_{24}p_{13} = \frac{\xi}{4},$$

has no solutions for $u = 5$. Proceeding with $u \in (-2, 5)$ we find solutions for p_{13} and p_{24} . The condition that p_{13} is positive restricts u to the interval $(-2, u_1)$ with $u_1 = \frac{8}{3} - \frac{2}{3}\sqrt[3]{19}$.

In step (iv) the requirement that the determinant $s_{13}^2 - 4p_{13}$ is non-negative gives the restriction $u \in [0, u_1]$. For these values of u we find the solutions in (9).

Resonance 1 : 2 : 2 To $(\lambda_1, \lambda_2, \lambda_3) = (\frac{4}{9}, \frac{4}{9}, \frac{1}{9})$ corresponds $(\xi, \eta) = (\frac{16}{729}, \frac{8}{27})$. In Fig. 15 it is hard to see whether it is in the region described in (51). A direct computation shows that $\eta > 2\xi + \frac{1}{4}$, so the fiber is empty.

If we carry out the steps in the computational scheme, the set of values that η_2 may have becomes empty when we check whether $d_{24} \geq 0$.

Resonance 1 : 1 : 2 With $(\lambda_1, \lambda_2, \lambda_3) = (\frac{2}{3}, \frac{1}{6}, \frac{1}{6})$ we have $(\xi, \eta) = (\frac{1}{54}, \frac{1}{4})$. The corresponding point in Fig. 15 seems to be on the boundary of the region for a non-empty fiber. Indeed, it turns out that $T(\xi, \eta)$ is exactly 0.

Following the computational scheme the expression for d_{13} in terms of η_2 turns out to be non-positive for $\eta_1 \in (0, \frac{1}{16})$, with a zero only at $\eta_2 = \frac{1}{18}$. This leads to the solution

$$(a_1, \dots, a_4) = \left(\frac{1}{12}, \frac{2 - \sqrt{2}}{12}, \frac{1}{12}, \frac{2 + \sqrt{2}}{12} \right). \tag{55}$$

It is invariant under the substitution [13] in the dihedral group. See Fig. 16.

Resonance 1 : 3 : 6 For $(\lambda_1, \lambda_2, \lambda_3) = (\frac{18}{23}, \frac{9}{46}, \frac{1}{46})$ we have $(\xi, \eta) = (\frac{81}{24334}, \frac{369}{2116})$. The corresponding point in Fig. 15 is to the left of the dashed line. This indicates that the fiber contains open curves.

Fig. 16 The fiber for the resonance 1 : 1 : 2 in spherical coordinates. The *thick point* corresponds to the vector in (55), the *other points* are its translates under elements of D_4 . The *curved line* indicates the boundary of the region with positive coordinates

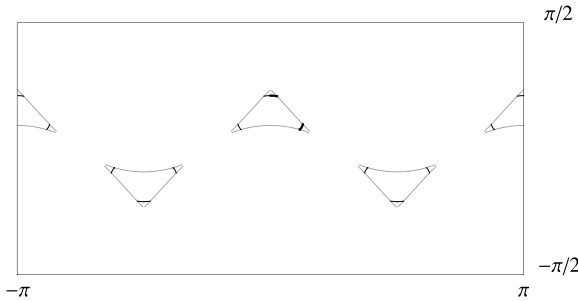
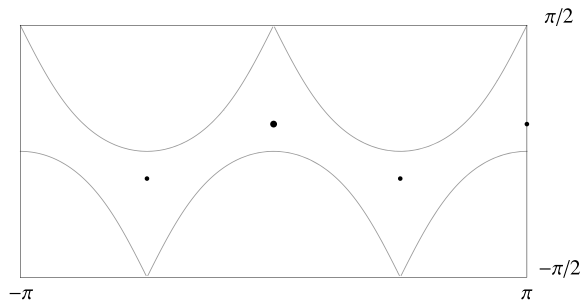


Fig. 17 The fiber for the resonance 1 : 3 : 6 in spherical coordinates. The interior of the *four triangles* correspond to the region with positive coordinates. The fiber consists of *twelve open curves*, three in each *triangle*. The computational scheme determines the thickly drawn part of the fiber. It consists of two components: the lower one is open at both of its end points; the upper one is open at one side, and ends at the point invariant under the permutation [1, 3]

The computational scheme gives solutions for

$$\eta_2 \in \left[\frac{11}{1058}, h_2 \right) \cup (h_3, h_4),$$

with algebraic numbers $h_2 \approx .112814$, $h_3 \approx .0501346$, $h_4 \approx .0548411$. For $\eta_2 = \frac{11}{1058}$ we find a point that is invariant under the permutation $[1, 3] \in D_4$. Figure 17 illustrates the fiber.

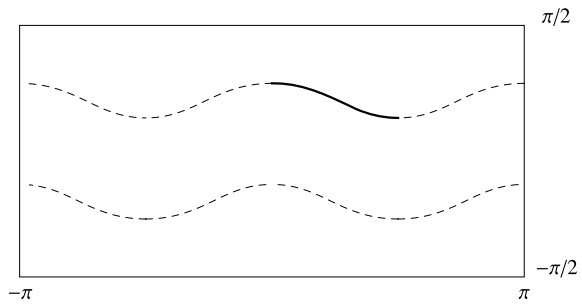
Resonance 2 : 3 : 4 For $(\lambda_1, \lambda_2, \lambda_3) = (\frac{16}{29}, \frac{9}{19}, \frac{4}{29})$ we have $(\xi, \eta) = (\frac{576}{24389}, \frac{244}{841})$. The corresponding point in Fig. 15 is in the region where the fiber is compact. All a_j are positive on the ellipsoid for $\eta = \frac{244}{841}$.

The computational scheme gives a family of solutions depending on $\eta_2 \in [\frac{42}{841}, \frac{99}{1682}]$. The end points give symmetric solutions: $a_1 = a_3$ for $\eta_2 = \frac{42}{841}$, and $a_2 = a_4$ for $\eta_2 = \frac{99}{1682}$. In Fig. 18 we see that the fiber consists of two closed curves.

A.3 Transformation matrices for the resonance 1 : 2 : 3

In Sect. 3.4 we computed functions $u \mapsto a_j(u)$, $1 \leq j \leq 4$, on the interval $[0, u_1)$ as diagonal elements of a diagonal matrix $A_4(u)$ such that $A_4(u)C_4$ has eigenvalues $\frac{9}{14}, \frac{4}{14}, \frac{1}{14}, 0$. For the transformation to eigenmodes of the Hamiltonian we need in Sect. 3.6 a family of orthogonal matrices $u \mapsto U(u)$ such that $U(u)$ diagonalizes $A_4(u)^{1/2}C_4A_4(u)^{1/2}$. For any specific value of u such orthogonal matrices can be found numerically. Here we indicate how we obtained a symbolic description.

Fig. 18 The fiber for the resonance 2 : 3 : 4 in spherical coordinates. The *thick line* corresponds to the solutions obtained by the computational scheme. The *dashed lines* are formed by the translates under D_4 of the computed part. In this case all points on the ellipsoid have positive coordinates



Lemma A.6 Let A_4 be a positive diagonal matrix with diagonal elements a_1, \dots, a_4 . Let λ be an eigenvalue of $A_4 C_4$ such that $\lambda \neq 2a_j$ for $1 \leq j \leq 4$. Put

$$\mu_j = \frac{1}{2 - \lambda/a_j}.$$

Then

$$(\mu_1(\mu_2 + \mu_4), \mu_2, \mu_3(\mu_2 + \mu_4), \mu_4)$$

is an eigenvector of $A_4 C_4$ for the eigenvalue λ .

Proof We have

$$C_4 - \lambda A^{-1} = \begin{pmatrix} \mu_1^{-1} & -1 & 0 & -1 \\ -1 & \mu_2^{-1} & -1 & 0 \\ 0 & -1 & \mu_3^{-1} & -1 \\ -1 & 0 & -1 & \mu_4^{-1} \end{pmatrix}.$$

We try to solve $(C - \lambda A^{-1})v = 0$ with $v = (p, x, q, y)$. The first and third lines give $x + y = \mu_1^{-1}p = \mu_3^{-1}q$. Similarly, we get $p + q = \mu_2^{-1}x = \mu_4^{-1}y$. Since λ is an eigenvalue of $A_4 C_4$ there are non-zero solutions, for which x and y both have to be non-zero. So there is a solution with $x = \mu_2$. Then we obtain the vector in the lemma. \square

Now we take for a_j the expressions in (9). It is clear that $2a_j(u) - \lambda_i$ is not identically zero in u for any of the eigenvalues $\lambda_1, \lambda_2, \lambda_3$, and $\lambda_4 = 0$, and any a_j . So we obtain vectors $v_i(u)$, $1 \leq i \leq 4$, that are eigenvectors of $A_4(u)C_4$ for the eigenvalue λ_i for generic values of u .

The vectors $w_i = A_4(u)^{-1/2}v_i$ are eigenvectors of $A_2(u)^{1/2}C_4A_4(u)^{1/2}$. Since the four eigenvalues are different, the w_i are orthogonal. We take $\tilde{w}_i = n_i^{-1}w_i$ with $n_i = \sqrt{w_i \cdot w_i}$ to get an orthonormal basis. There is the freedom to choose the sign. We multiply \tilde{w}_1 with -1 , to get consistency with our earlier computations.

The \tilde{w}_i can be chosen as the columns of the orthogonal matrix $U(u)$. Then the vectors

$$\tilde{v}_i = A_4(u)^{1/2}\tilde{w}_i = n_i^{-1}v_i(u)$$

are the columns of the transformation matrix $L(u) = A_4(u)^{1/2}U(u)$.

The construction of the v_i allows the components to have singularities. The orthonormalization removes all singularities, so the matrix elements of $L(u)$ are continuous functions on

$[0, u_1)$, given by algebraic expressions. An explicit expression for the other transformation matrix $K(u) = A_4(u)^{-1/2}U(u) = A_4(u)^{-1}L(u)$ follows easily.

References

1. Born, M.: *The Mechanics of the Atom*. G. Bell and Sons, London (1927) (transl. J.W. Fisher, rev. D.R. Hartree, orig. German ed. 1924)
2. Bourbaki, N.: *Éléments de Mathématique, Groupes et algèbres de Lie*, Chap. 4, 5 et 6. Hermann, Paris (1968)
3. Bruggeman, R., Verhulst, F.: Near-integrability and Recurrence in FPU chains with alternating masses (2016, submitted)
4. Christodoulidi, H., Efthymiopoulos, Ch., Bountis, T.: Energy localization on q -tori, long-term stability, and the interpretation of Fermi-Pasta-Ulam recurrences. *Phys. Rev. E* **81**, 6210 (2010)
5. Christov, O.: Non-integrability of first order resonances in Hamiltonian systems in three degrees of freedom. *Celest. Mech. Dyn. Astron.* **112**, 149–167 (2012)
6. Devaney, R.L.: Homoclinic orbits in Hamiltonian systems. *J. Differ. Equ.* **21**, 431–438 (1976)
7. Fermi, E., Pasta, J., Ulam, S.: Los Alamos Report LA-1940, in “E. Fermi, Collected Papers” 2, pp. 977–988 (1955)
8. Ford, J.: *Phys. Rep.* **213**, 271–310 (1992)
9. Galgani, L., Giorgilli, A., Martinoli, A., Vanzini, S.: On the problem of energy partition for large systems of the Fermi-Pasta-Ulam type: analytical and numerical estimates. *Physica D* **59**, 334–348 (1992)
10. Hoveijn, I., Verhulst, F.: Chaos in the 1 : 2 : 3 Hamiltonian normal form. *Physica D* **44**, 397–406 (1990)
11. Poincaré, H.: *Les Méthodes Nouvelles de la Mécanique Céleste*, 3 vols. Gauthier-Villars, Paris (1892, 1893, 1899)
12. Rink, B., Verhulst, F.: Near-integrability of periodic FPU-chains. *Physica A* **285**, 467–482 (2000)
13. Rink, B.: Symmetry and resonance in periodic FPU-chains. *Commun. Math. Phys.* **218**, 665–685 (2001)
14. Sanders, J.A., Verhulst, F., Murdock, J.: *Averaging Methods in Nonlinear Dynamical Systems*, 2nd edn. Applied Mathematical Sciences, vol. 59. Springer, Berlin (2007)
15. Udawadia, F.E., Mylapilli, H.: Energy control of inhomogeneous nonlinear lattices. *Proc. R. Soc. A* **471**, 20140694 (2015)
16. Verhulst, F.: *Methods and Applications of Singular Perturbations*. Springer, Berlin (2005)
17. Verhulst, F.: *Henri Poincaré, Impatient Genius*. Springer, Berlin (2012)
18. Verhulst, F.: Integrability and non-integrability of Hamiltonian normal forms. *Acta Appl. Math.* **137**, 253–272 (2015)
19. Verhulst, F.: Near-integrability and recurrence in FPU cells. *Int. J. Bifurc. Chaos* **26**, 1650230 (2016). doi:[10.1142/S0218127416502308](https://doi.org/10.1142/S0218127416502308)
20. Weinstein, A.: Normal modes for nonlinear Hamiltonian systems. *Invent. Math.* **20**, 47–57 (1973)